ANNUAL REVIEWS

Annual Review of Earth and Planetary Sciences

Submarine Landslides and Their Tsunami Hazard

David R. Tappin[1,2]

[1]Environmental Science Centre, British Geological Survey, Keyworth, Nottingham NG12 5GG, United Kingdom; email: drta@bgs.ac.uk

[2]Department of Earth Sciences, University College London, WC1E 6BS, United Kingdom

Annu. Rev. Earth Planet. Sci. 2021. 49:551–78

First published as a Review in Advance on March 15, 2021

The *Annual Review of Earth and Planetary Sciences* is online at earth.annualreviews.org

https://doi.org/10.1146/annurev-earth-063016-015810

Keywords

tsunami, submarine landslide, hazard, earthquake, volcano, strike-slip fault

Abstract

Most tsunamis are generated by earthquakes, but in 1998, a seabed slump offshore of northern Papua New Guinea (PNG) generated a tsunami up to 15 m high that killed more than 2,200 people. The event changed our understanding of tsunami mechanisms and was the forerunner to two decades of major tsunamis that included those in Turkey, the Indian Ocean, Japan, and Sulawesi and Anak Krakatau in Indonesia. PNG provided a context to better understand these tsunamis as well as older submarine landslide events, such as Storegga (8150 BP); Alika 2 in Hawaii (120,000 BP), and Grand Banks, Canada (1929), together with those from dual earthquake/landslide mechanisms, such as Messina (1908), Puerto Rico (1928), and Japan (2011). PNG proved that submarine landslides generate devastating tsunamis from failure mechanisms that can be very different, whether singly or in combination with earthquakes. It demonstrated the critical importance of seabed mapping to identify these mechanisms as well as stimulated the development of new numerical tsunami modeling methodologies. In combination with other recent tsunamis, PNG demonstrated the critical importance of these events in advancing our understanding of tsunami hazard and risk. This review recounts how, since 1998, understanding of the tsunami hazard from submarine landslides has progressed far beyond anything considered possible at that time.

- For submarine landslide tsunamis, advances in understanding take place incrementally, usually in response to major, sometimes catastrophic, events.

- The Papua New Guinea tsunami in 1998, when more than 2,200 people perished, was a turning point in first recognizing the significant tsunami hazard from submarine landslides.
- Over the past 2 to 3 years advances have also been made mainly because of improvements in numerical modeling based on older tsunamis such as Grand Banks in 1929, Messina in 1908, and Storegga at 8150 BP.
- Two recent tsunamis in late 2018, in Sulawesi and Anak Krakatau, Indonesia, where several hundred people died, were from very unusual landslide mechanisms—dual (strike-slip and landslide) and volcanic collapse—and provide new motivations for understanding these tsunami mechanisms.
- This is a timely, state of the art review of landslide tsunamis based on recent well-studied events and new research on older ones, which provide an important context for the recent tsunamis in Indonesia in 2018.

INTRODUCTION

Over the past 20 years, major advances in understanding the mechanisms of tsunami generation have resulted in an improved recognition of their variability, hazard, and risk. These advances resulted mainly from a number of major, if not devastating, tsunamis together with revisions of older ones. Of critical importance, however, were new technologies available to study the different tsunami mechanisms, which included high-resolution global systems of navigation and seismic networks, high-resolution seabed mapping, improved data recording and storage, and numerical tsunami models. Earthquakes generate the majority (~80%) of tsunamis and are the best-known mechanism of tsunami generation, especially the Indian Ocean tsunami of 2004 in which more than 220,000 people died. Although they cause fewer fatalities than earthquakes, a number of significant tsunamis resulted from submarine landslides; before 1998, the best known were those of the Grand Banks in 1929 and prehistoric Storegga at 8150 BP (**Figure 1**).

A new, raised awareness of the tsunami hazard from submarine landslides (e.g., Lee et al. 2003, Løvholt et al. 2015) resulted after July 1998, when the northern coast of Papua New Guinea (PNG) was devastated by waves of up to 15 m that caused more than 2,200 fatalities (Kawata et al. 1999). The associated earthquake was not a tsunami earthquake and, with a magnitude M_w 7.1, could not explain the tsunami wave elevations and pattern of inundation (Synolakis et al. 2002, Tappin et al. 1999). During responsive marine surveys, from multibeam echosounder (MBES) bathymetry seismic and sediment cores offshore the devastated area, a small (6 km^3) sediment failure was identified as a slump. From the ad hoc shipboard numerical tsunami modeling, the slump was confirmed as the most likely tsunami mechanism (Tappin et al. 1999); however, this interpretation was initially controversial (Geist 2000).

This review addresses tsunamis generated from submarine landslides, singly and in association with earthquakes; how these differ from those generated solely by earthquakes; and their impacts. The focus is on those events where there is corroborative evidence of tsunamis, rather than all submarine landslides that are potentially tsunamigenic but without supporting evidence. This review shows why their hazard was not recognized before the 1998 PNG event and how this led to the identification of the hazard from submarine landslides. It also reports on new research on pre-1998 landslide events along passive and convergent margins that, benefiting from the realization at PNG and new technology and understandings, improves and refines our understanding of their associated tsunamis and their hazard. It then addresses the very recent tsunamis of Palu, Sulawesi, and Anak Krakatau in 2018 and why submarine landslide tsunamis today are still less

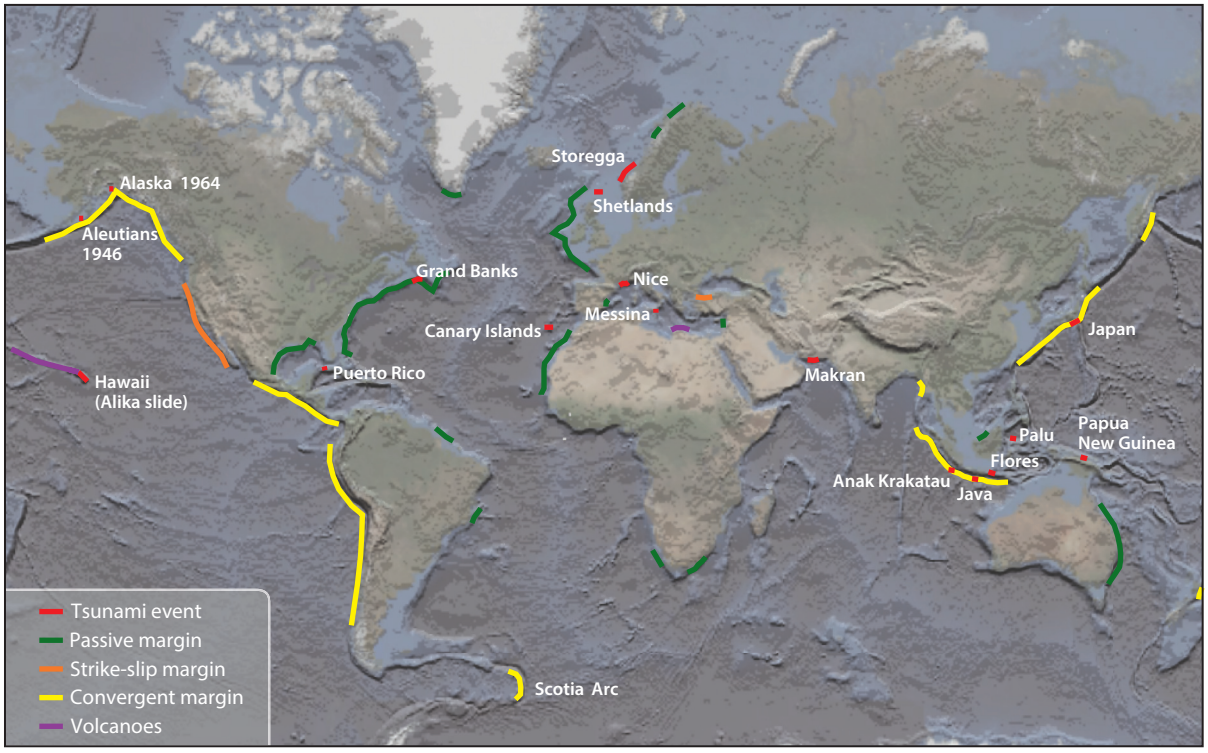

Figure 1

Global distribution of mapped oceanic margins and identified submarine landslide-generated tsunamis or where these contributed to the event—for example, Canary Islands (e.g., 170,000 BP), Alika 2 in Hawaii (125,000 BP), Storegga (8,150 BP), Messina (1908), Puerto Rico (1918), Grand Banks (1929), Makran (1946), Aleutians-Unimak (1946), Alaska (1964), Nice (1979), Flores (1992), Papua New Guinea (1998), Japan (2011), Palu (Sulawesi; 2018), and Anak Krakatau (2018). Figure adapted from Tappin (2017).

well understood than those from earthquakes. The review ends with future approach suggestions to address this deficit.

UNDERSTANDING OF LANDSLIDE TSUNAMIS BEFORE PAPUA NEW GUINEA IN 1998

Tsunamis from submarine landslides are unusual, with limited fatalities compared to those from earthquakes. Before the PNG event, based on theoretical considerations, landslides were considered less efficient than earthquakes in generating high-elevation tsunamis (e.g., LeBlond & Jones 1995). This was surprising because there were a number of well-described submarine landslide tsunamis, such as Grand Banks, Flores Islands, and Storegga. The 1929 Grand Banks landslide was known to be triggered by the associated earthquake (Murty 1977). The 1992 Flores Island tsunami was mainly generated by an earthquake that also triggered a landslide (Yeh et al. 1994). Although it was not proven at the time, there was also evidence for a submarine landslide contribution to the Aleutian tsunami of 1946 (Johnson & Satake 1997). Prehistoric landslide tsunamis include Storegga, dated at 8150 BP (Dawson et al. 1988, Harbitz 1992) in the North Atlantic, and the collapse of some Hawaiian volcanoes, such as Alika 2 in the Pacific, dated at ~120,000 BP (Moore & Moore 1988). Both Storegga and Alika 2 were large-volume landslides, with no

evidence for an associated earthquake contribution, although Storegga was earthquake triggered (Bryn et al. 2005). Other submarine landslide tsunamis were those triggered by the great Alaskan earthquake of 1964, which claimed 45 lives at Seward and Valdez (**Figure 1**). Landslides consequential to human activities include those at Skagway, Alaska, in 1964, which killed one person (Kulikov et al. 1996), and at Nice airport in 1979, when a coastal collapse triggered a tsunami with one fatality (Assier-Rzadkieaicz et al. 2000).

The evidence for these tsunamis varies. There were eyewitness accounts at Grand Banks, Alaska, and Flores Islands (Clague 2001, Plafker et al. 1969, Ruffman & Hann 2006, Yeh et al. 1993). At Grand Banks, the landslide had been mapped (e.g., Piper et al. 1988), and the earthquake was discounted and the landslide mechanism confirmed from seismograms (Bent 1995). At Flores Islands, there were field survey coastal observations that identified highly elevated tsunami runups of 26 m at Riangkroko (Yeh et al. 1993). A numerical model of the tsunami showed that the earthquake could not explain these runups (Imamura et al. 1995).

With prehistoric events, the evidence for landslide tsunamis was from sediments deposited as these flooded the land (e.g., Dawson et al. 1988, Felton et al. 2000, Moore & Moore 1988). For Storegga, the sediments were first discovered several meters above present sea level on the east coast of Scotland (Dawson et al. 1988), and their identification stimulated and validated numerical tsunami modeling (Harbitz 1992). In Hawaii, the tsunami interpretations were not as clear-cut. Sediments proposed as deposited by the tsunami from the Alika 2 volcanic collapse were up to 325 m above present sea level, but a numerical tsunami model concluded that the proposed landslide mechanism did not generate these elevations (Johnson & Mader 1994). There was additional controversy over the tsunami from Alika 2 because the on-land elevated sediment had previously been interpreted as deposited from sea-level highstands (Grigg & Jones 1997, Stearns 1978).

THE PAPUA NEW GUINEA TSUNAMI IN 1998

Initial Results and Interpretations

The PNG tsunami struck late in the evening of July 17, 1998 (Kawata et al. 1999). The tsunami was geographically focused and flooded 30 km of the coast (**Figure 2**). The M_w 7.1 earthquake was too small to generate the recorded tsunami waves of up to 15 m, and it was not a tsunami earthquake according to the definition of Newman & Okal (1998) based on the discriminant of E/M_0. In addition, the aftershock distribution indicated it was a shallow-, not steeply-dipping, thrust, so it was unlikely to have been the tsunami mechanism (Hurukawa et al. 2003). There was no warning of the tsunami except the earthquake shaking—hence the more than 2,200 fatalities. This loss of life was the greatest from a tsunami in more than 20 years, the most since the Moro Gulf earthquake event in the Philippines in August 1976, which caused more than 8,000 fatalities, most (~90%) in the tsunami.

The most likely location of the earthquake epicenter was west of the main area of destruction and close to land (**Figure 2**) (**https://www.usgs.gov/centers/pcmsc/science/descriptive-model-july-17-1998-papua-new-guinea-tsunami?qt-science_center_objects=0#qt-science_center_objects**). From field surveys (Kawata et al. 1999), the geometry of rupture, as inferred from the location of the main shock and aftershocks, was hard to reconcile with the concentration of the devastation to the east of the earthquake epicenter. The 18-min delay between the earthquake shaking and tsunami impact also indicated that another mechanism was responsible for the event. There were three tsunami waves, with the first causing a withdrawal of the sea and interpreted as a leading depression wave (Kawata et al. 1999). Succeeding waves were closely spaced, arriving within minutes, and were much smaller than the first. These descriptions

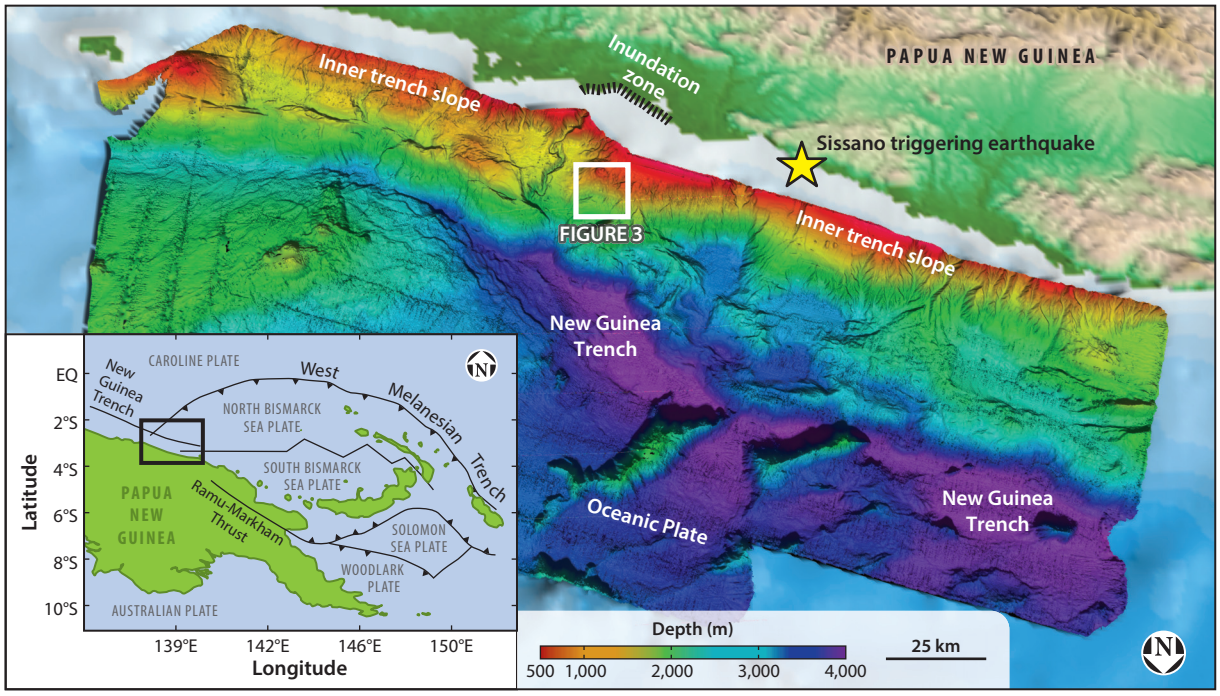

Figure 2

Digital elevation model of seafloor relief offshore of northern Papua New Guinea looking south (vertical exaggeration times 4). The region is a convergent margin with tectonic erosion resulting in collapse along the inner trench and submarine landsliding. The white box shows the slump location in **Figure 3**. The inset shows the location of the mapped area in **Figure 3** and the regional tectonic framework. Figure adapted from Tappin (2010).

indicated a highly dispersive wave train generated by a submarine landslide rather than the individual waves generated by successive strong components of a sequential seismic rupture. Without marine hydroacoustic data (MBES and seismic) to investigate the event, the tsunami mechanism at that time remained unknown.

Marine Surveys and First Results on the Tsunami Mechanism

Because of the large number of fatalities and the uncertainty over the tsunami mechanism, Japan offered to carry out two marine surveys to acquire seabed bathymetry, seismic and sediment samples north of PNG in the region of the tsunami mechanism. This was the first time after a major tsunami that responsive marine surveys were carried out, and in early 1999, during a 2-week survey, 19,000 km^2 of 12-kHz MBES bathymetry were acquired offshore of northern PNG (**Figure 2**). In addition, offshore of the devastated area, 4.2-kHz sub-bottom seismic data were also acquired together with four 7-m sediment piston cores (Tappin et al. 1999). From these data the area offshore of northern PNG was interpreted as experiencing significant subduction erosion, resulting in subsidence and collapse of the inner trench slope that formed the northern margin of the overriding plate. In the area most devastated by the tsunami, 25 km offshore of the Sissano Lagoon, an amphitheater-shaped seabed feature of about 10 km^2 was identified (**Figure 3**). This feature was interpreted as being formed by a sediment slump with a volume of 6 km^3. Sediment cores on and around the slump sampled fine-grained cohesive clays, confirming the likely slump

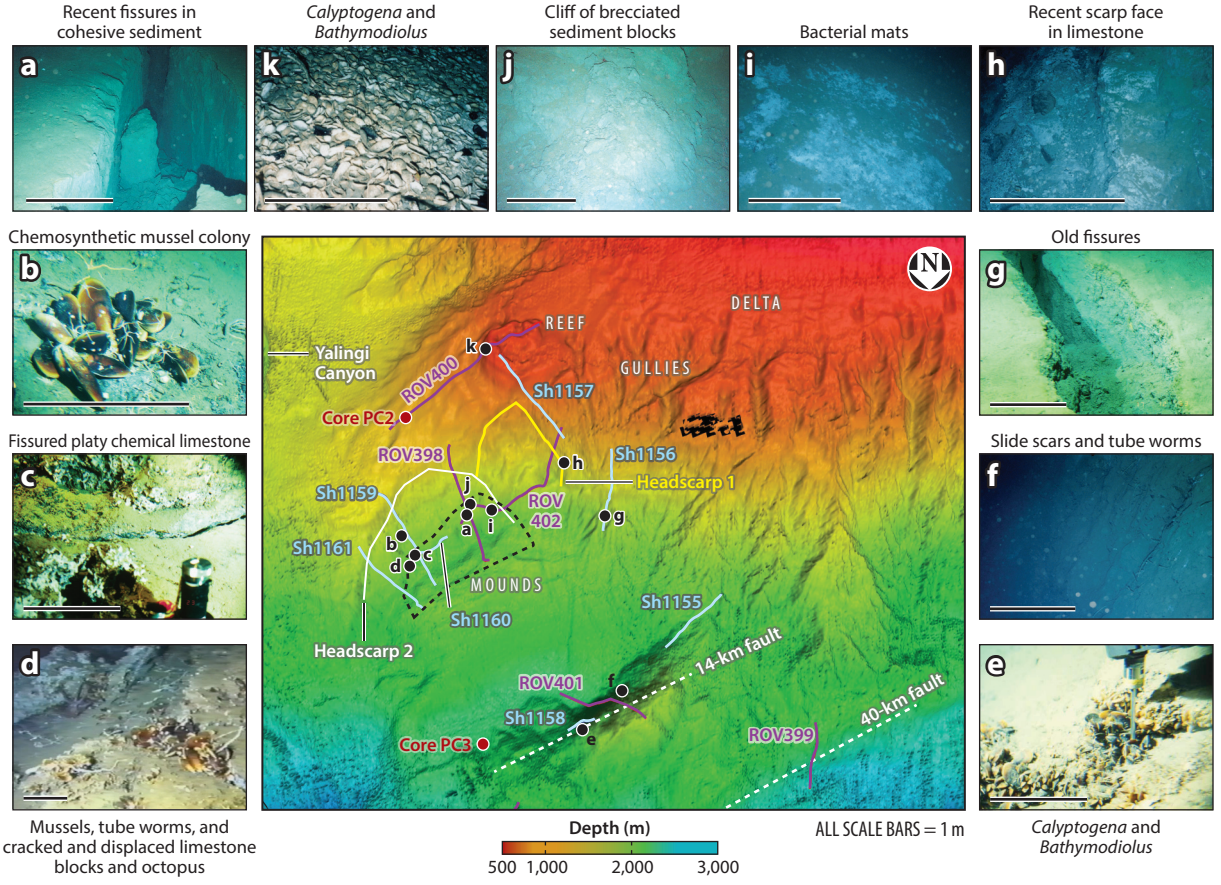

Figure 3

The amphitheater-shaped area offshore of the Sissano Lagoon, Papua New Guinea, with the main morphologic features labeled and photographs of significant seabed features. This is the location of the slump that caused the July 1998 tsunami, with the white and yellow lines defining the two headscarps, with the white the most recent slump of July 1998. Purple lines indicate remotely operated vehicle (ROV) traverses; light blue lines indicate Shinkai (Shi) manned submersible dive traverses. The black dashed line defines the most concentrated region of the biological communities. Figure adapted with permission from Tappin (2020).

failure mechanism. From still and video seabed photography acquired by remotely operated vehicles, fresh fissures and fluid expulsion (**Figure 3**) from the slump indicated it to be very recent.

The first two marine surveys provided the initial indications that the slump in the amphitheater was the most likely tsunami mechanism (Tappin et al. 1999). Preliminary, ad hoc, numerical tsunami models devised onboard the survey vessels confirmed that an earthquake could not generate the local tsunami, as the faults mapped had normal movement or were not long enough. The tsunami modeled from the slump generated runups of 5 m, much less than the maximum 15 m recorded, but this was still considered the most likely tsunami mechanism. Later in 1999, multichannel seismic (MCS) data acquired during a US-funded survey confirmed the presence of a slump up to 760 m thick within the amphitheater (Sweet & Silver 2003). In early 2000 and 2001, two Japanese-funded marine surveys deployed a manned submersible, Shinkai 3000, and acquired single-channel seismic data. The submersible dives within the amphitheater confirmed recent movement of the slump from sharply defined fissures, concentrations of cold-water

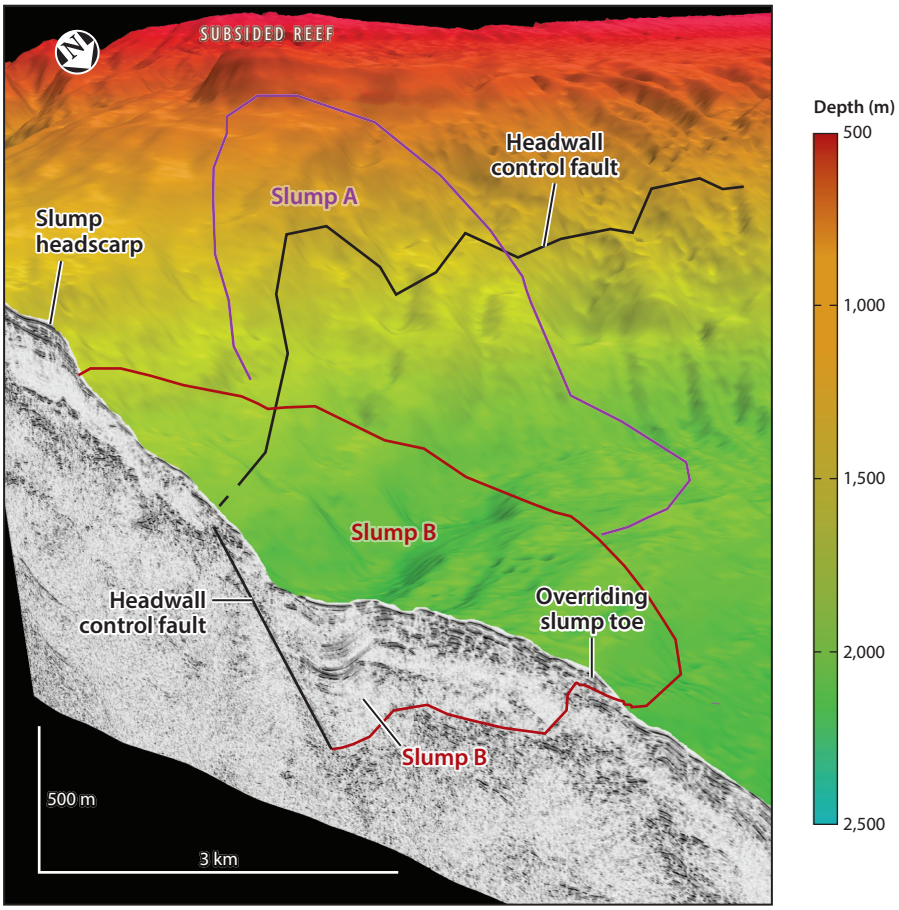

Figure 4

Three-dimensional cutaway section of the Papua New Guinea slump showing seabed morphology and subseabed seismic viewed from the northeast (vertical exaggeration times 3). There are a number of slumps at this location identified by Slump A and B, with B the event of July 1998. The slump failed along the headwall fault, with a horizontal travel distance of 800 m. Figure adapted from Tappin et al. (2008) (CC BY-NC-SA 2.5).

chemosynthetic communities, and fluid expulsion (**Figure 3**) from the seabed (Tappin et al. 2001). The seismic data confirmed the extent of the slump (**Figure 4**).

PAPUA NEW GUINEA: CONTROVERSY AND WAKE-UP CALL

Immediately after the first two marine surveys, when the initial results on the slump tsunami origin were published, some doubt was expressed over this interpretation (Geist 2000). This was mainly because, although there were previously recognized landslide tsunamis, they were not as devastating as that of PNG, and tsunamis numerically modeled from landslides were rare (e.g., Harbitz 1992). There were a number of aspects to this view. First, there were differences in how earthquakes and landslides generate tsunamis, with landslides believed to be too slow and too small. Second, the numerical tsunami models available in 1998 were not suitable for nonseismic

mechanisms. And third, the number of different submarine landslide failure mechanisms made modeling challenging (see Geist 2000). Subsequent numerical modeling based on additional marine geological and geophysical data and improved numerical models (Tappin et al. 2001, 2008) validated the tsunami slump mechanism. These were based on improved and validated modeling programs with the initial condition (wavemaker) from Tsunami Open and Progressive Initial Conditions System (TOPICS) software, which provided the vertical landslide displacements as outputs, as well as a characteristic tsunami wavelength and a characteristic tsunami period. The dispersive physics of landslide tsunamis were addressed using the Boussinesq propagation models, GEOWAVE (Watts et al. 2003) and the later development, FUNWAVE. These numerical models initially provided tsunami wave elevations offshore, not on-land runups, but later modeling provided tsunami wave elevations at the coast (**Figure 5**). This was a significant improvement over earlier simulations using tsunami source and (nondispersive) shallow-water tsunami propagation simulations.

How Earthquakes and Submarine Landslides Generate Tsunamis

Tsunamis are gravity-driven water waves generated at the water/air interface from a vertical perturbation of the water column. Their velocities are determined by $c = \sqrt{gh}$, where c is celerity, g is gravity (9.8 m/s^2), and h is water depth. The deeper the water, the faster the tsunami travels. For earthquakes, there are three phases of a tsunami: (*a*) initial wave generation from seabed movement, (*b*) surface wave collapse and propagation (travel) through the ocean, and (*c*) on-land incursion or runup (wave elevation at the coast) when the tsunami strikes and flows across land. Earthquake tsunami-generation models assume initial vertical water surface deformation to be equal to that at the seabed, as water is virtually incompressible, and for the rise time of most earthquakes, the long-wave phase velocity in the ocean is slow enough so that water displacement of the tsunami is considered instantaneous. There are slight modifications to the tsunami wave field for earthquakes of slow rupture duration (tsunami earthquakes). Seabed deformation is calculated from earthquake fault parameters using theoretical deformation models, such as by Okada (1985).

Submarine landslides generate tsunamis in a similar manner to earthquakes by a vertical displacement of the seabed that creates a similar displacement at the sea surface (**Figure 6**), but there are several major differences. Landslide displacements are much slower, with velocities of tens to hundreds of meters rather than 3–4 km/s for earthquakes, with the longer source times making numerical tsunami modeling of landslides challenging. The areas of seabed disturbance from submarine landslides are also much smaller than those of earthquake rupture, reducing their tsunamigenic potential. Landslide tsunamis are strongly oriented along the direction of landslide movement, and there are many different landslide mechanisms, with the different morphologies depending mainly on sediment type (Hampton et al. 1996). In the context of tsunami generation, the kinematics of landslide failure can be considered either as blocks or slumps that, on failing, in large part maintain their integrity, or as translational, where the sediment disintegrates. The recognition that tsunami generation by landslides is dependent on their failure mechanism modifies the three elements of earthquake tsunami generation because there is a precursor to tsunami generation, which is the landslide failure.

Before PNG, theoretical numerical modeling of tsunamis from submarine landslides was based on a Bingham-type fluid flow, analogous to a translational mechanism, where large blocks traveling downslope disintegrated to form turbidity currents (Geist 2000, Hampton 1972). Modeling of solid block landslides at the time of the PNG tsunami was in its infancy (Watts 1998). Numerical tsunami-generation models were initially based on depth-averaged wave equations that represented immiscible liquids or water as a Bingham plastic (Jiang & LeBlond 1992, 1994).

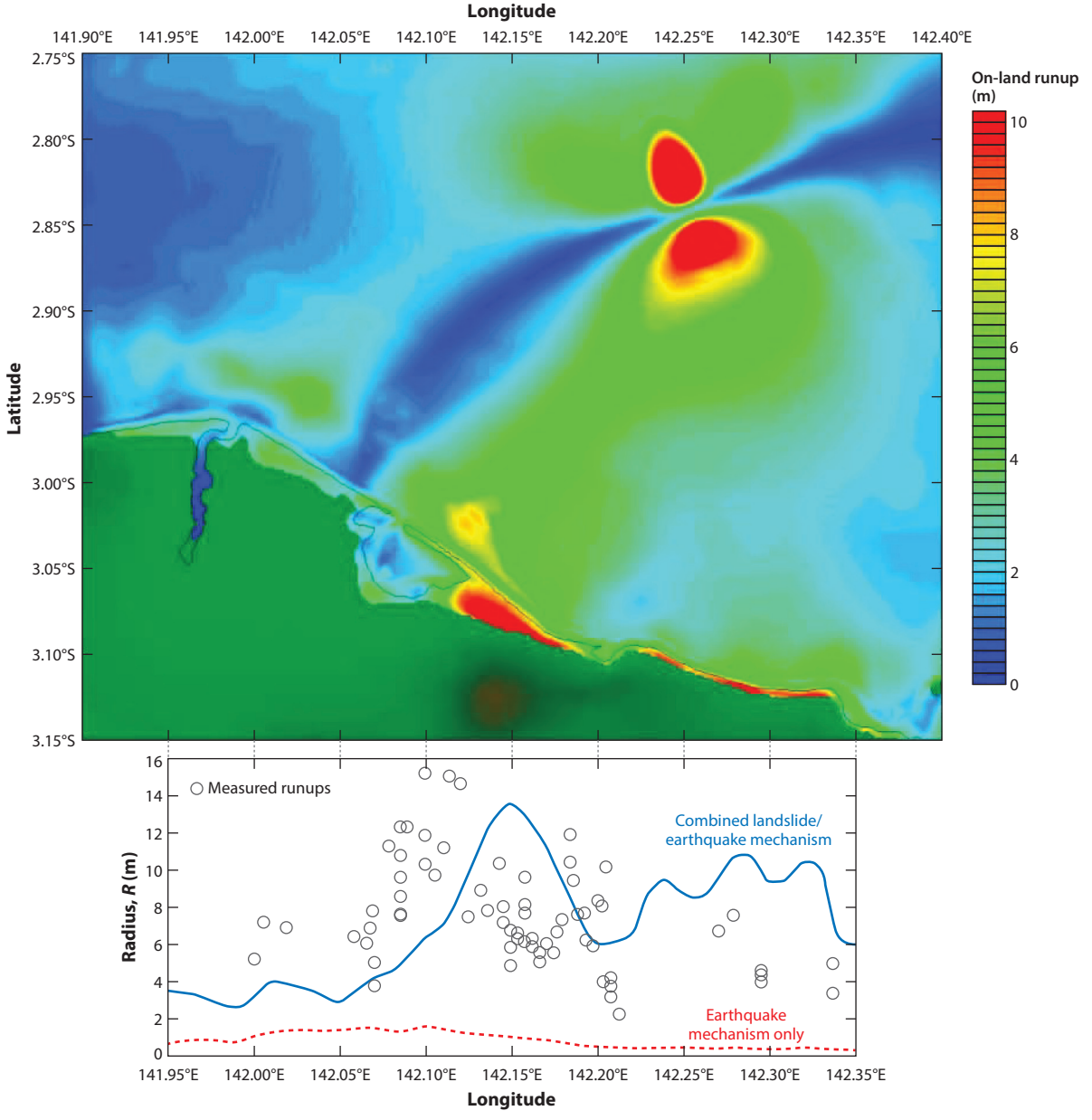

Figure 5

Numerical simulation of the 1998 Papua New Guinea tsunami source from Tsunami Open and Progressive Initial Conditions System (TOPICS) software 1.2 combined with the fully nonlinear and dispersive model FUNWAVE with on-land runup. Note in the lower figure the offset between the modeled and measured, which is due to the slight misorientation of the landslide failure direction. Figure adapted from Tappin et al. (2008) (CC BY-NC-SA 2.5).

Depth averaging accurately applies to tsunami generation from earthquakes, but it is questionable when applied to landslide tsunamis because it does not allow for vertical fluid accelerations, which are important during submarine landslide motion and tsunami generation (Grilli et al. 2002). In 1998, landslide constitutive equations used in numerical models were largely untested

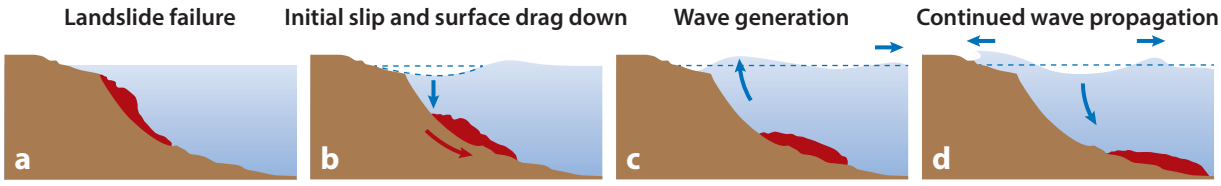

Figure 6

How submarine landslides generate tsunamis: (*a*) landslide failure, (*b*) initial slip and surface drag down above the rear of the landslide, (*c*) positive and negative wave generation, and (*d*) landslide movement halts and continued wave propagation. Note how, as the slide travels downslope, it elevates the sea surface above the front and pulls down the sea surface to the rear, analogous to earthquake-generated tsunamis but much slower. Figure adapted from Platf. Promot. Early Warn. (2006).

by laboratory experiments or by case studies (Tappin et al. 2008). Submarine landslide models were idealized and not based on geological data (which were generally not available). There was no established method of merging geological data with numerical landslide models, and there was little appreciation of the complexity of modeling tsunamis generated from the different submarine landslide mechanisms. For all these reasons, submarine landslides were considered to be ineffective at generating significant tsunamis (Geist 2000, LeBlond & Jones 1995). When the PNG tsunami happened and the earthquake was an unlikely mechanism, the major challenge was in understanding how the relatively slow-moving slump submarine landslide generated the tsunami.

POST–PAPUA NEW GUINEA TSUNAMI DEVELOPMENTS

Despite initial reservations over the landslide mechanism of the PNG tsunami (Geist 2000), as the results were published, there was increased interest in the landslide tsunami hazard, especially for events such as Storegga, Grand Banks, and Hawaii, where there was already existing research and great interest in their potential hazard.

The Prehistoric Storegga Landslide Tsunami

The Storegga landslide (**Figure 7**) was one of the largest in the world, with a volume of 2,400–3,200 km^3 (Haflidason et al. 2004), an area of 95,000 km^2, and a runout distance of 300 km. The landslide generated a turbidite that covered an extensive area of the North Atlantic. It failed retrogressively on a very shallow slope of 1–2°. There were a number of landslides at the Storegga location, each taking place at the end of the 120,000-year glacial/interglacial climate cycle that drives the waxing and waning of the ice sheets and the associated changes in sea level. This cyclicity at Storegga also controls landslide triggering (Bryn et al. 2005). The slide had been identified much earlier (Bugge et al. 1987) than PNG, with the associated tsunami identified from sediments deposited on the east coast of Scotland as it flooded the land (Dawson et al. 1988). Discovery of these sediments motivated the first attempt at numerically modeling a submarine landslide tsunami (Harbitz 1992). The failure model used was based on a slide architecture derived from hydroacoustic data, such as seismic and bathymetry data, and the tsunami on-land runup was validated from the east coast Scotland sediments. When the PNG tsunami struck, a major investigation into the Storegga tsunami was just beginning because of the 1997 discovery of the Ormen Lange gas field beneath the landslide headwall. There was concern that, although landslide tsunamis can be triggered naturally, they might also be caused by human-induced activities, such as the proposed extraction of gas from beneath the Storegga headscarp (Solheim et al. 2005). The PNG tsunami confirmed that this was undoubtedly possible.

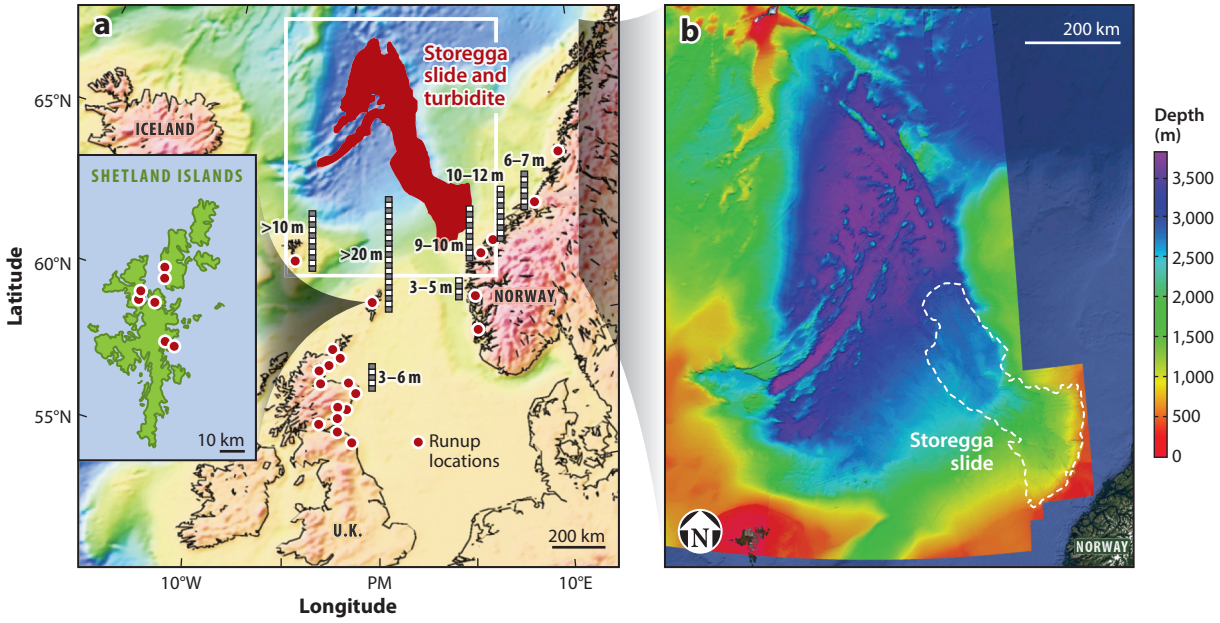

Figure 7

The Storegga, Norway, landslide and tsunami. Panel *a* shows landslide location and elevation of tsunami runups on surrounding coasts, adapted from Bondevik et al. (2003). Panel *b* shows a digital elevation model of the landslide (*white dotted line*) and the resulting turbidite covering the purple seabed region to the northwest. Figure adapted from EMODnet Bathymetry Consort. (2018).

Numerical models of the Storegga tsunami postdating PNG (Bondevik et al. 2005, Hill et al. 2014) were significant improvements on the 1992 research (Harbitz 1992), as they were based on a more comprehensive data set of geophysics and coring of the landslide headscarp (Bryn et al. 2005). In addition, validation of later numerical models was from more extensive tsunami on-land sediment runup data from Norway (Bondevik et al. 1997), the Faroe Islands (Grauert et al. 2001), the Shetland Islands (Bondevik et al. 2003), and mainland Scotland (Smith et al. 2007). The later numerical models reproduced the maximum tsunami runups identified from the Shetland sediments, which were up to at least 20 m above present sea level and probably higher (~30 m) above sea level at the time of the slide (Bondevik et al. 2005). Even with the large-scale resources expended on Storegga, there were still uncertainties over the relationships between the climate controls on the triggering of the landslide and tsunami generation (Solheim et al. 2005).

Most recently, further numerical modeling of large-volume landslides on the Norwegian margin including Storegga and Trænadjupet, located farther north, resulted in further advances in tsunami model development. There has also been increased interest in the tsunami hazard in the North Atlantic from very large-volume landslides, with the likelihood of their triggering possibly increased by global warming (Hill et al. 2014; Løvholt et al. 2015, 2017). These studies have led to new insights into landslide tsunamis that include the following: First, large-volume landslides do not necessarily generate tsunamis commensurate with their size. Second, tsunamis generated from long runout distances of translational large-volume landslides such as Storegga may not be dispersive (Glimsdal et al. 2013). And third, retrogressive failure is a critical control on tsunami generation because it results in a smaller initial elevation wave compared to landslides that fail from the top. Overall, the research demonstrates the importance of landslide morphology in tsunami modeling both in representing the failure mechanism and in the resulting initial tsunami elevation and

extent. It is critically important, therefore, to use appropriate landslide mechanisms in numerical tsunami modeling. Other important factors controlling tsunami generation include slide velocity, slide volume, failure mechanism, water depth, and slide distance from shoreline. Further, blocks and slumps are impulsive events, and it is their velocity that is most important in initial tsunami generation, whereas with translational landslides it is their acceleration (Løvholt et al. 2015). Generally, translational landslides are larger volume with longer runout distances compared to blocks and slumps. These large-volume landslides are generally considered retrogressive, failing from the bottom up, a mechanism that, as noted above, reduces their tsunamigenic potential. The research confirms that even large-volume landslides may produce tsunamis of only modest size and that the frequency dispersion of large-volume landslide tsunamis may not be as important as previously believed. This is because the tsunami wavelengths generated by these events are longer and akin to those of earthquakes, so they can travel farther without losing energy, unlike smaller-volume landslides.

The Hawaiian Giant Submarine Landslides

The PNG tsunami resulted in further research on the Hawaiian giant submarine landslides (GSLs) (**Figure 1**) to ascertain their tsunami hazard by focusing on the origin of the elevated tsunami deposits found on the Hawaiian Islands, from new numerical tsunami modeling of the collapse of the 120,000 BP Alika 2 event (**Figures 1** and **8**). Detailed sedimentology and age dating on the sedimentary deposits on Lana'i and Moloka'i, Hawaii (Moore 2000, Rubin et al. 2000), seemed not to resolve whether they were deposited from highstands (Stearns 1978) or tsunamis, as proposed by Moore & Moore (1988). Research on similar deposits on the Big Island of Hawaii (McMurtry et al. 2004a), however, demonstrated that these most likely resulted from a tsunami with an elevation of ~500 m above sea level at the time of deposition. This interpretation was based on the 120,000 BP age of both the Big Island on-land deposits and the offshore Alika 2 GSL, which indicated a strong genetic link. Numerical tsunami modeling of the Alika landslide confirmed this as the source of the on-land sediments, producing local runup elevations of hundreds of meters (McMurtry et al. 2004b). It demonstrated that the Hawaiian large-volume volcanic GSLs were a potential tsunami hazard, with their triggering related to global warming and cooling climate changes over the past hundreds of thousands of years.

The Grand Banks Tsunami of 1929

Until 1998, research on the Grand Banks event (**Figure 1**) had mapped the landslide (Heezen & Ewing 1952, Piper et al. 1988), but a numerical model of the tsunami was not attempted until much later (Fine et al. 2005). The research was stimulated by the landslide tsunamis in the Flores Islands in 1992, Turkey in 1999, Skagway, and PNG. Twenty-eight people drowned in the Grand Banks tsunami, which was caused by an earthquake-triggered landslide (Heezen & Ewing 1952, Fine et al. 2005). The earthquake's strike-slip mechanism and magnitude, M_w 7.2, were too small to generate the tsunami (Bent 1995). Strike-slip earthquakes rarely cause the seabed vertical movement necessary to generate large tsunamis. At shallow water depths, the earthquake broke submarine telephone cables, but sequential, deeper water breaks resulted from sediment movement from turbidites moving downslope. The sediment failure covers an area of 5,200 km^2 with a sediment volume of 200 km^3 deposited over 150,000 km^2 (Piper et al. 1988). The initial failure was small but triggered numerous overlapping, thin failures. As with Storegga, the slide was translational and retrogressive. Although nearly 100 years old and well-studied, up until recently the landslide was mapped only with backscatter data. From this and seabed sediment samples, the

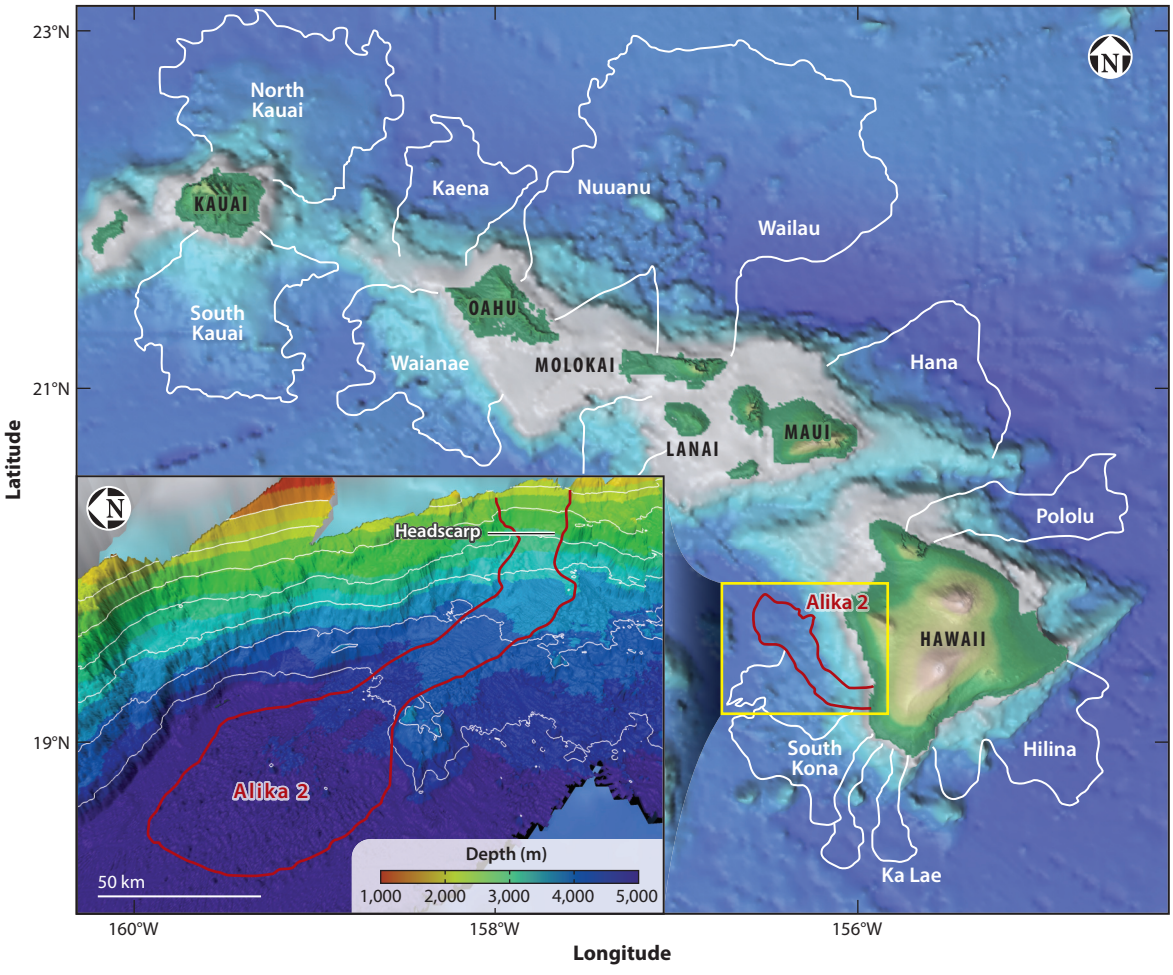

Figure 8

Hawaiian giant landslides: seabed morphology, locations, and extents. The inset shows the Alika 2 landslide from 120,000 BP (*yellow box*). The Alika 2 landslide, with a volume of 350 km^3, caused a tsunami up to 500 m high on the nearby island of Hawaii. Figure adapted from Tappin (2010).

landslide mechanism and morphology have been interpreted. It was not until this century, however, that MBES bathymetry was acquired to map the landslide in detail, and these data provided a basis for new numerical tsunami modeling (Løvholt et al. 2018, Mosher & Piper 2007, Schulten et al. 2018, Zengaffinen et al. 2020).

Previous modeling of Grand Banks (Fine et al. 2005) was based on a viscous incompressible fluid and a nondispersive physical model. Even using the new MBES and seismic data, however, the landslide was difficult to define (Mosher & Piper 2007) because there was no evidence of a single large event, a major headscarp, or a debris lobe. From the new data, the landslide proved to be a complex association of shallow seabed failures (Schulten et al. 2018), with the surficial sediment failures concentrated along deep-water escarpments. These failures comprise widely distributed, translational, retrogressive slumps that liquefied into debris flows, which rapidly evolved into a massive channelized turbidity current. The slump headscarps are 100 m in elevation, and their

deep-water location and retrogressive failure made them unlikely to be the main tsunami mechanism. This suggested that the shallow-water slumps, with their localized fault scarps, were the main cause. Numerical tsunami modeling based on the new hydroacoustic data confirms this interpretation and shows that the shallow-water slumps generated the elevated tsunami runups observed locally in Newfoundland and that the translational landslides generated the longer-period waves observed in the far field (Løvholt et al. 2018).

RECENT DEVELOPMENTS: DUAL-MECHANISM TSUNAMIS

Over the past 5 to 10 years, there has been a further resurgence in interest in landslide tsunamis. In large part this has resulted from new developments in numerical models of submarine landslide tsunamis that are based on their different failure mechanisms and that generate dispersive tsunamis. These new models have resulted in improvements beyond solid block landslides modeled as earthquakes. A major contributory factor has been the increased availability of MBES bathymetry, which provides much-improved, high-resolution imaging of seabed morphology. As described above, older events such as Grand Banks and Storegga have been revisited, together with Messina in 1908 and Puerto Rico in 1918. In March 2011, however, another catastrophic tsunami struck that, despite the warning from the Indian Ocean 7 years prior, arrived unexpectedly in another completely different context and devastated the country that was best prepared for tsunamis: Japan.

Japan Tsunami, March 11, 2011

The 2011 Japan tsunami was another challenging event because, although the earthquake was large at M_w 9.1, there is evidence that this on its own may not have generated all of the recorded tsunami. The tsunami struck the east coast of Honshu Island, but the earthquake magnitude was not predicted, so the tsunami was far higher and more destructive than expected. More than 18,000 people perished. Because of its large magnitude, the earthquake was immediately interpreted as the single tsunami mechanism, but this could not explain elevated (40 m) and focused tsunami runups along the Sanriku coast on Honshu Island north of latitude 39°N (**Figure 9**) (e.g., Fujii et al. 2011, MacInnes et al. 2013). In addition, inversion of tsunami waveforms could not reproduce the timing and high-frequency content of the tsunami recorded at the nearshore GPS buoys located offshore of Sanriku nor the timing of the dispersive wave train at the Deep-Ocean Assessment and Reporting of Tsunamis (DART) buoy #21418 located 600 km off the coast (e.g., Grilli et al. 2013).

The high-frequency content of the tsunami waveforms recorded by bottom sensors offshore of the northern region of the rupture, together with the elevated runups north of the main rupture, suggested there could be an additional mechanism, a submarine landslide. Support for an additional submarine landslide mechanism for the 2011 tsunami was first proposed by Kawamura et al. (2012). Based on a comprehensive analysis of the event and numerical modeling, Tappin et al. (2014) suggested this additional submarine landslide mechanism was located due east of the highest tsunami runups (**Figure 9**). From MBES bathymetry, a landslide was identified to the east of the high on-land runups, much farther north than the landslide proposed by Kawamura et al. (2012). Numerical modeling of the tsunami from the dual (earthquake/submarine landslide) mechanism with the landslide at the location proposed by Tappin et al. (2014) reproduced reasonably well the elevated (40 m) tsunami waves along the Honshu coast better than the earthquake on its own, especially in the north of the inundated area, in the Sanriku region.

The 2011 Japan dual-mechanism tsunami, however, remains controversial. Recently published numerical earthquake tsunami simulations, based on inversion of tsunami wave data (Lay 2018,

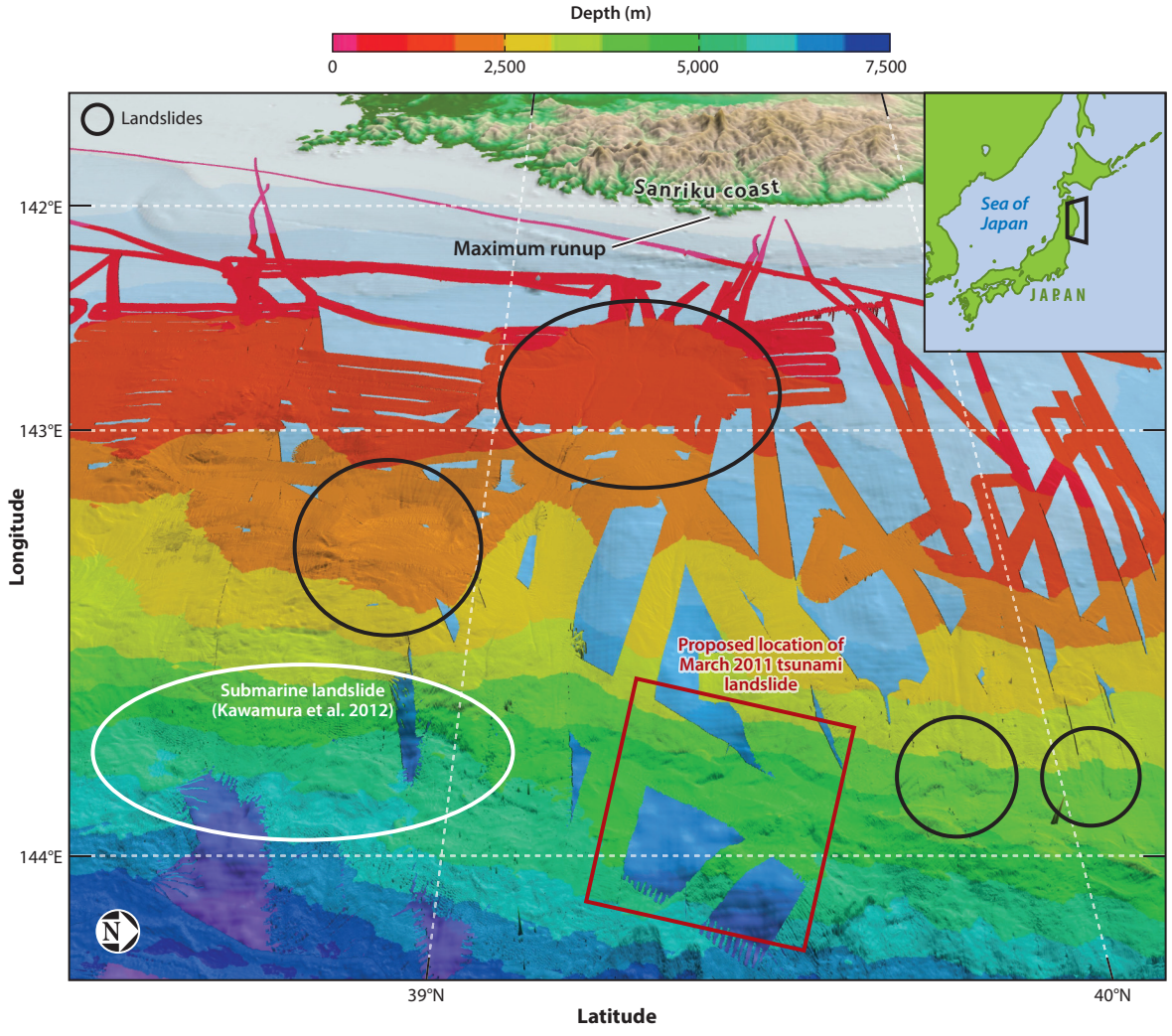

Figure 9

Submarine landslides in the region offshore the northern Honshu (Sanriku) coast from pre-March 2011 Japan Marine Science and Technology Center bathymetry. The landslide proposed as the source of the highest-elevation observed on-land tsunami runup/inundations (around 39.5°N) is located directly offshore to the east of these. Figure adapted from Tappin et al. (2014).

Yamazaki et al. 2018), propose seabed movement in the region of the submarine landslide, but the mechanism is not defined. To test the additional landslide mechanism for the 2011 Japan tsunami proposed by Tappin et al. (2014), bathymetric data in the region of their landslide were acquired in 2017 (Fujiwara et al. 2017). These data revealed no evidence for a large submarine landslide displacement at the location proposed. Notwithstanding the absence of a major landslide at this location from before and after 2011, MBES bathymetry and MCS seabed failures are identified on the northern margin of the 2011 earthquake rupture and farther north (Boston et al. 2017, Tappin et al. 2014). Most recently, from pre-2011 seismic data, seabed slumping has been identified in deeper waters below the landslide proposed by Tappin et al. (2014), which is proposed as possibly contributing to the 2011 tsunami (Nakamura et al. 2020). A major hindrance to identifying seabed

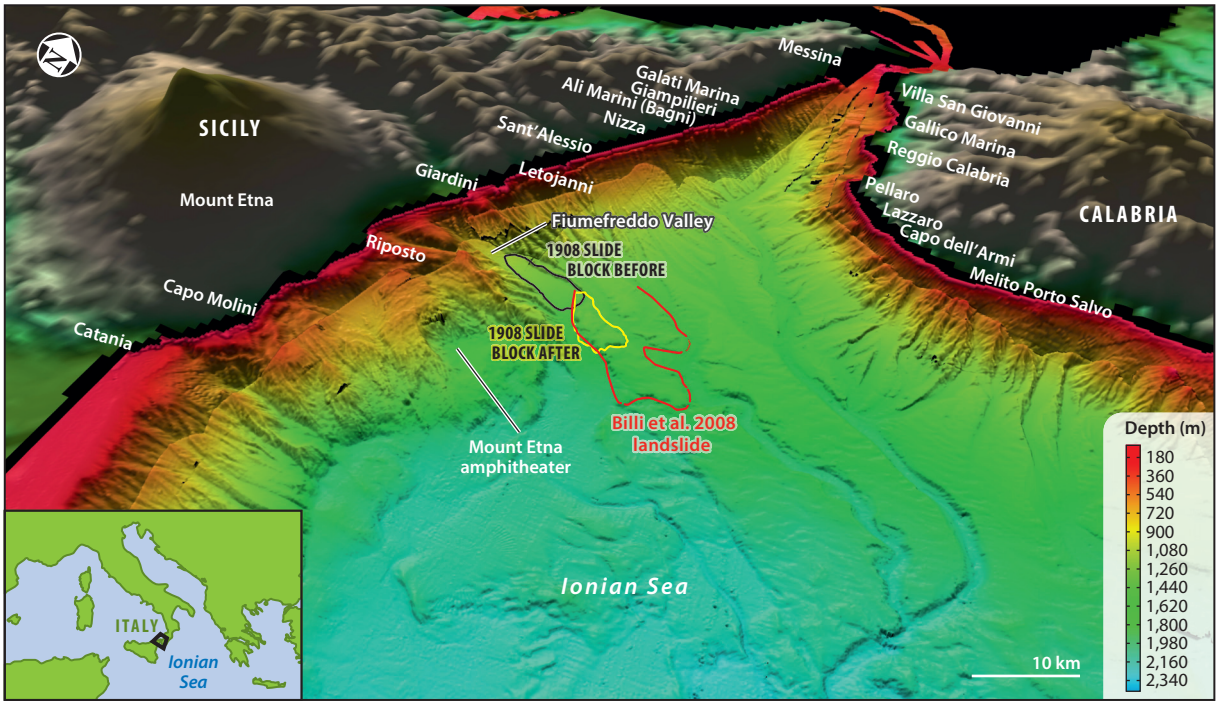

Figure 10

The Messina tsunami. Digital elevation model of the Ionian Sea between Sicily and Calabria showing the landslide block that contributed to the 1908 Messina tsunami. [Multibeam echosounder bathymetry from Marani et al. (2004).] The red outline marks the location of the landslide identified by Billi et al. (2008); the black and yellow outlines mark the proposed location of the 1908 submarine landslide, before and after failure, respectively. Although new numerical tsunami models support the landslide block as contributing to the tsunami in the south, additional landslides are still required in the north. Figure adapted with permission from Schambach et al. (2020b).

movement in the region north of 39.5°N is the lack of post-event MBES bathymetry, which could answer whether there are submarine landslides here triggered by the 2011 earthquake. There are landslides in this region identified on the pre-2011 MBES data (**Figure 9**), but post-event MBES bathymetry is necessary to identify what their movement is.

Dual-Mechanism Tsunamis: Other Events

Japan raised the profile of dual-mechanism tsunamis where earthquakes and submarine landslides might be involved, and, with MBES bathymetry increasingly available, it is possible in many instances to address the mechanisms of these events. The tsunamis of Messina in 1908 (**Figure 10**) and Puerto Rico in 1918 have been subject to controversy for more than 100 years (López-Venegas et al. 2008, Schambach et al. 2020b). With Puerto Rico, there is historical evidence for landsliding from the breakage of submarine telegraph cables. MBES bathymetry also shows evidence of a submarine landslide that, together with numerical tsunami modeling, now supports the landslide mechanism of the tsunami (López-Venegas et al. 2008).

With the 1908 Messina event, seabed sediment movement was originally identified from submarine cable breakages (Ryan & Heezen 1965) and coastal landslides (Baratta 1910, Omori 1909). Soon after the event took place, Omori (1909) proposed seabed sediment movement at the margins and bottom of the Messina Strait as a possible contribution to the tsunami. The earthquake and

tsunami were catastrophic, with ~60,000 fatalities, but the rupture was restricted to north of the Ionian Sea in the Messina Strait, so it cannot explain tsunamis up to 12 m in elevation much farther south along the east coast of Sicily and on the south coast of Calabria. A landslide was identified offshore of Mount Etna (Billi et al. 2008), and numerical modeling based on hypothetical mechanisms supported this interpretation (Favalli et al. 2009). More recently, a slide block was identified offshore of Mount Etna from MBES bathymetry. This landslide, together with the earthquake, was the basis for numerical simulations that reproduced the tsunami over much of the southern Messina Strait and Ionian Sea region (Schambach et al. 2020b). The block landslide mapped offshore Mount Etna is at a location consistent with earlier studies (e.g., Billi et al. 2008) but is a fairly rigid-block-slide rather than a translational submarine mass failure (SMF). The new tsunami modeling (Schambach et al. 2020b) is based on higher-resolution grids and more accurate bathymetry and topography than in earlier work. Runups and travel times agree well with observations, except for runups on either side of the Messina Strait north of the block landslide that are still underpredicted. The new modeling of this event confirms that an additional mechanism or mechanisms are required in the north to explain runups in the Messina Strait region. The additional mechanism(s) may be the coastal landslides on Sicily and Calabria described by Omori (1909) and Baratta (1910).

RECENT EVENTS IN INDONESIA IN 2018

Toward the end of 2018, two destructive tsunamis struck Indonesia, one in Sulawesi in September and a second in the Sunda Straits between Java and Sumatra in December. The mechanisms of these events were very different, with the first associated with a strike-slip earthquake and the second associated with a volcanic eruption. The Sulawesi tsunamis were up to 10–11 m in elevation, much larger than expected from the earthquake mechanism, but observations from field studies suggested that coastal landslides could have contributed to the tsunami. At Anak Krakatau, a flank collapse generated the tsunami, with most data published on the subaerial features but little on the submarine part (Hunt et al. 2021, Priyanto et al. 2021).

Both recent Indonesian tsunamis flag the hazard from nonseismic tsunami mechanisms and how still few case studies there are. Anak Krakatau is important because it is the first volcanic flank collapse tsunami since Krakatau in the late nineteenth century and the first major event where there is an opportunity to utilize modern technology to map both the subaerial and the submarine parts of the collapse. The last major eruption tsunami was at the same location, the famous event of 1883, with 36,000 fatalities.

Sulawesi (Palu) Tsunami, September 28, 2018

A M_w 7.5 supershear earthquake struck Central Sulawesi, Indonesia, on September 28, 2018, rapidly followed by a destructive tsunami in Palu Bay (Bao et al. 2019, Socquet et al. 2019). The earthquake was predominantly strike-slip, which could not explain the maximum 11-m runups recorded in the southern part of the bay. This interpretation was confirmed by most published earthquake models, which predicted limited vertical deformation. Some papers identified several meters of vertical uplift, not in the bay but outside and farther north (Song et al. 2019). Others (Ulrich et al. 2019) suggested that the strike-slip mechanisms along steeper sides of the bay resulted in an apparent greater uplift, such as the mechanism proposed by Tanioka & Satake (1996).

Responsive field surveys after the event identified numerous small coastal landslides (**Figure 11**), which offered an alternative tsunami mechanism (Arikawa et al. 2018, Muhari et al. 2018, Nakata et al. 2020). There was subsequent debate over whether the tsunami was generated by an earthquake, coastal landslides, or a combination of both. Early publications on the tsunami

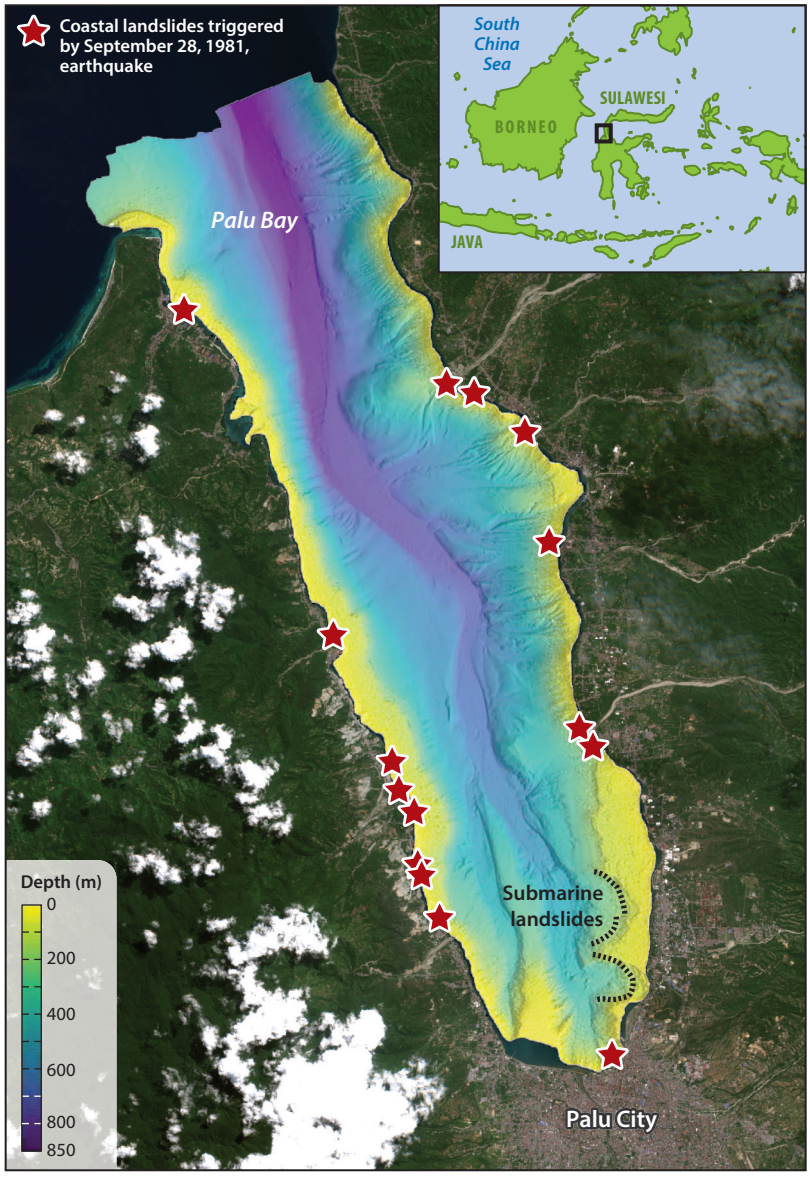

Figure 11

Map of the Palu Bay, Sulawesi, area showing seabed morphology, location of coastal landslides, and submarine landslides in the southeast. The bathymetry is a merge of data from Frederik et al. (2019) and Liu et al. (2020). Recent numerical simulations of the tsunami by Schambach et al. (2020a) suggest that it was caused by a combination of the strike-slip earthquake, the coastal landslides, and a submarine landslide in the southeast of the bay. The figure includes modified Copernicus Sentinel-2 data 2018.

were inconclusive in this regard, with some identifying the earthquake as explaining most tsunami observations and others disregarding the earthquake contribution entirely and focusing solely on landslide sources, but these were based on hypothetical landslides not confirmed by post-tsunami bathymetric surveys (Pakoksung et al. 2019).

The most recent research (Schambach et al. 2020a) models the tsunami from a combination of earthquake ruptures (based on Jamelot et al. 2019, Socquet et al. 2019, Ulrich et al. 2019), which vary in their basis and complexity, and coastal landslides mapped from field and video evidence of the tsunami impact, together with marine bathymetric surveys (**Figure 11**). It uses a combination of two numerical models generating the tsunami and propagating the waves, the three-dimensional (3D) nonhydrostatic wave model NHWAVE and the 2D Boussinesq wave model FUNWAVE-TVD. These new models are critically important because they address the physics of wave frequency dispersion, which is necessary for modeling landslide-generated tsunamis. The coastal landslides were modeled in NHWAVE as granular material. The results from the combined earthquake and coastal landslide models reproduce the recorded and observed tsunami runups around the bay except in the southeast, where there were the most elevated (11 m) runups. A major challenge in recreating the tsunamis was addressing the timing of impact from the local coastal landslides. And, for the first time with the Sulawesi event, there is reasonable agreement between the landslide plus earthquake models of Socquet et al. (2019) and Ulrich et al. (2019) and the timing of tsunami impact at several locations around the bay. The results of the modeling confirm that, to explain the tsunami in the southeast of Palu Bay, a local mechanism in addition to the earthquake is required, and that this is a small-volume submarine landslide located just offshore.

Anak Krakatau, December 22, 2018

At approximately 20:56 local time on December 22, 2018, Anak Krakatau volcano, in the Sunda Straits, Indonesia, experienced a major lateral collapse during a period of eruptive activity that began in June (Walter et al. 2019). The collapse, into the 250-m-deep caldera graben, located on the southwest flank of the volcano, generated a tsunami up to 80 m in elevation within the caldera, with runups of up to 13 m on the adjacent coasts of Sumatra and Java (Grilli et al. 2019) (**Figure 12**). There were 437 fatalities, the greatest loss of life in a volcanic tsunami since the catastrophic explosive eruption of Krakatau in 1883 and the sector collapse of Ritter Island in 1888. For the first time in more than 100 years, the event provided an opportunity to study a major volcanic tsunami with widespread loss of life and significant damage. The eruption of Anak Krakatau is closely linked to that of 1883 because the volcano developed within the remains of the Krakatau caldera largely destroyed in that cataclysmic event. From a submarine volcano in the northeast of the caldera, Anak Krakatau developed into a subaerial edifice, with a pre-2018 collapse height of about 335 m. The growth and collapse of Anak Krakatau was due to three reasons (Grilli et al. 2019): (*a*) its location above NNE-SSW-trending feeder vents that control volcanic activity of the volcano, (*b*) the location of Anak Krakatau on the northeast margin of the 250-m-deep graben in the west of the caldera, and (*c*) the gradual migration of Anak Krakatau toward the edge of the graben since the 1883 Krakatau eruption.

Based on hydroacoustic MBES and seismic data acquired in August, 2019, the landslide formed mainly of large blocks of subaerially erupted lavas (**Figure 13**) that were emplaced on friable submarine erupted pyroclastics, which were therefore inherently unstable (Hunt et al. 2021, Priyanto et al. 2021). The eruption triggered the collapse. As seen from pre- and post-event satellite images and aerial photography, 50% of Anak Krakatau volcano failed into the graben, causing a landslide with a submarine deposit volume of 0.214 ± 0.036 km^3. A landslide volume of 0.24 km^3, based on estimates predating the acquisition of the hydroacoustic data, was used to initialize a tsunami generation and propagation model with two different landslide rheologies (granular and fluid) (Grilli et al. 2019). Observations of a single tsunami with no subsequent waves are consistent with interpretation of landslide failure in a rapid single phase of movement, rather than a more piecemeal process, generating the tsunami, which reached nearby coastlines within ~30 min.

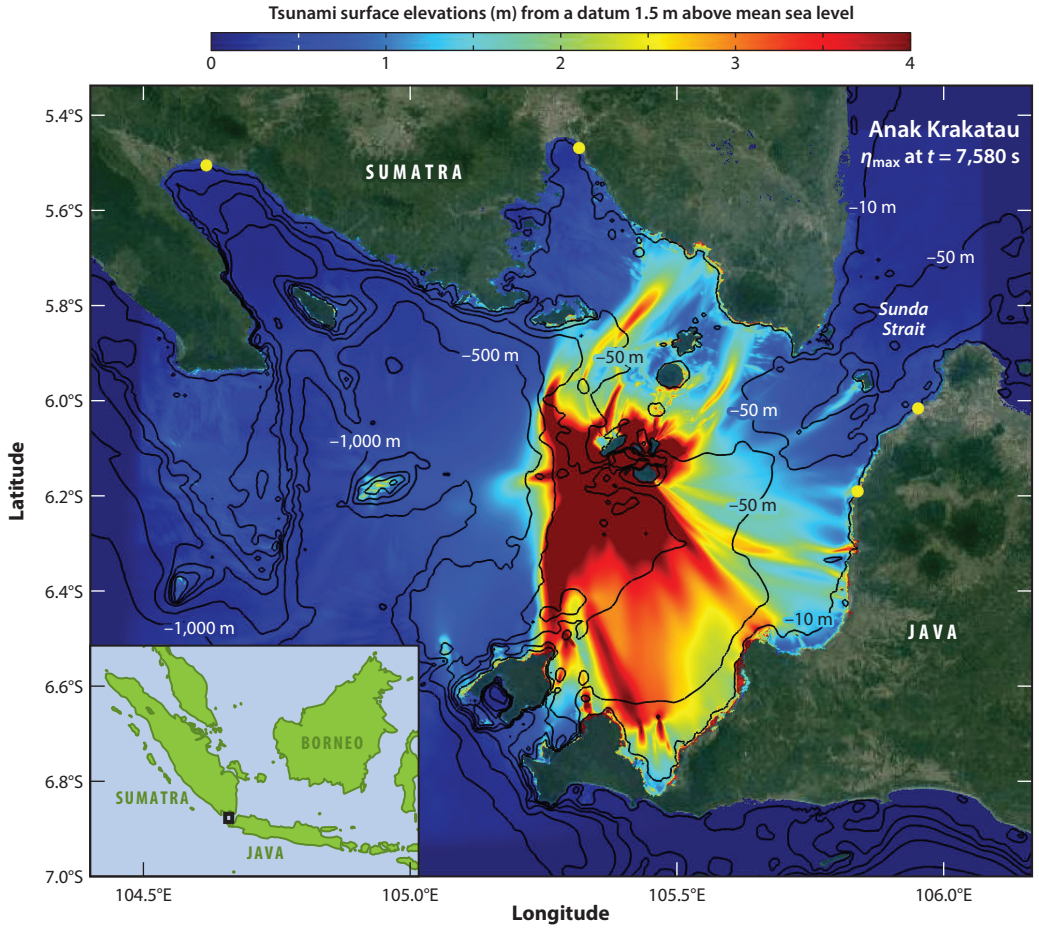

Figure 12

Tsunami surface elevations for Anak Krakatau collapse, using envelope of NHWAVE and FUNWAVE-TVD SE up to 7,610 s. The flank collapse volume was 0.24 km^3, and the initial tsunami was up to 80 m in elevation in the caldera and up to 13 m on surrounding coastlines. Figure adapted from Grilli et al. (2019). The image was produced using MATLAB version 2017b; the background topography is from Google Earth, **https://earth.google.com/web/**.

Both modeled rheologies successfully reproduce observed tsunami characteristics from post-event field survey results, tide gauge records, and eyewitness reports, suggesting the estimated landslide volume range is appropriate. The Anak Krakatau tsunami highlights the significant hazard from relatively small-scale lateral volcanic collapses, which can occur without any precursory signals and are an efficient and unpredictable tsunami source. The absence of precursory warning signals and the short travel time following tsunami initiation present a major challenge for mitigating tsunami coastal impact.

SUBMARINE LANDSLIDE TSUNAMIS: THE HAZARD REMAINS UNDEFINED

Before PNG, submarine landslides were not considered a major tsunami hazard, if they were considered at all. High-impact, low-frequency hazards such as earthquakes and tsunamis are a major

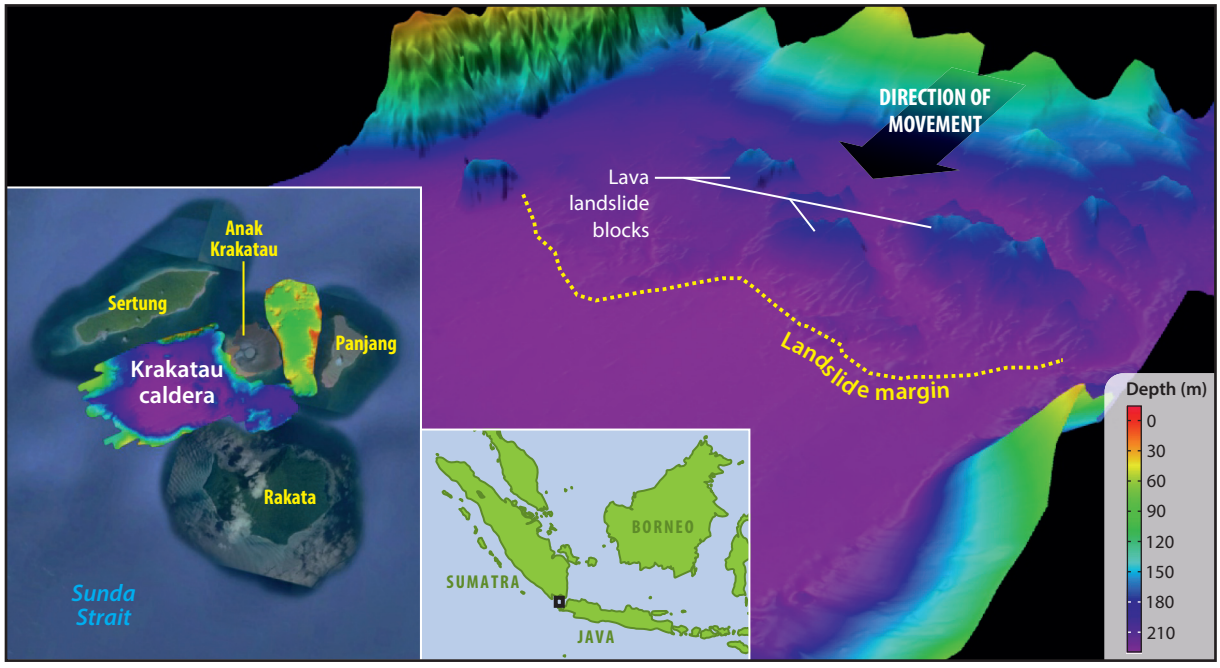

Figure 13

Digital elevation model of the landslide resulting from the eruption and collapse of Anak Krakatau in the Sunda Straits on December 22, 2018. The landslide did not disintegrate but formed large lava blocks, as seen in the figure; the deposit volume is 0.214 ± 0.036 km^3.

challenge because of the cost of investigation and their unpredictability. Major storms, for example, take place several times a year, but with events that strike on frequencies of 50 to 100 years, if not over longer time intervals, it takes a major disaster both to excite interest and to attract research funding. Where the hazard has not previously been recognized, as in 1998 with submarine landslide tsunamis, it is even more challenging. Even though submarine and subaerial landslide tsunamis had been known for many years, it took a major disaster, with more than 2,200 fatalities, to identify and raise the profile of the hazard. This is not too different from earthquake tsunamis. In the Indian Ocean tsunami in 2004, 220,000 people died. Of this total, 170,000 were in Aceh, close to the epicenter; without a warning system, there was no chance of evacuation. But the other 50,000 fatalities in India, Thailand, and Sri Lanka should not have happened because the tsunami took 2–3 h to reach their coastlines, enough time to warn and evacuate local populations. The last great earthquake before the Indian Ocean was Valdiva, on the west coast of South America, in 1960, so great earthquake science in 2004, in the context of the 40-year age gap, was significantly out of date. This resulted in the earthquake hazard in the Indian Ocean region not being considered and, in this context, being underestimated (Ruff & Kamamori 1980, Stein & Okal 2007). Because of this situation, whereas earthquakes off the west coast of South America were a well-established hazard, in the Indian Ocean they were not, so the magnitude of the 2004 earthquake and associated tsunami was a major surprise, with devastating consequences for local coastal populations.

Over the period since the 1998 PNG event, the tsunami hazard from submarine landslides has been increasingly well researched, generally accepted, and more widely recognized. After the initial controversy over the mechanism, the PNG event has been transformative in this major advance. The extensive mapping of continental margins shows that submarine landslides are

commonly found (**Figure 1**). The controls on submarine landslide tsunami generation, however, are complex and related to the global tectonic framework in which they occur as well as regional climate influences. Along passive margins and up until recently, mainly based on Storegga, passive margin landslide tsunamis were considered to have a strong climate control. The Storegga research suggests that landslide failure is related to sedimentation regimes controlled in part by the 120,000-year interglacial/glacial cycles, with triggering mainly from earthquakes. Recent research off Norway and northern Great Britain suggests that this climate influence may be applicable only to Storegga. The controls on landslides along convergent margins are not as well established but are probably dominated by local sedimentation regimes, with triggering from earthquakes.

Five years ago, only four major submarine landslide tsunamis had been identified, researched, and validated: Storegga, Grand Banks, PNG, and Japan (Tappin 2017). As evidenced here, over the intervening period, additional tsunamis have been identified as generated from submarine landslides or dual mechanisms. Older events, such as Grand Banks and Storegga, have been better studied and understood. Most recently, research on the Messina tsunami of 1908 demonstrates a submarine landslide contribution. Other events where there is a suspicion of a landslide influence—such as Makran in 1945, Aleutians in 1946, Alaska in 1964, Flores Islands in 1992, and Java in 2006—still require further research to understand their specific mechanisms and so remain enigmatic.

Along convergent margins, one of the most tantalizing challenges is the definition of tsunami earthquakes, where the tsunamis generated are much larger than expected from their associated earthquake surface wave magnitudes. These mechanisms were identified in 1972 (Kanamori 1972) based on two events: Sanriku in 1896 and the Aleutians tsunami of 1946. An important proviso, identified by Kanamori (1972), was that these tsunamis alternatively could have been associated with submarine landslides; as noted above for the 1946 event, evidence published later suggested that a submarine landslide was probably involved (Johnson & Satake 1997). There is evidence in the region offshore of the 1896 event for submarine landslides (Tappin et al. 2014), and it has now been demonstrated that the local tsunami of the Aleutians in 1946 was also likely generated by a landslide (Fryer et al. 2004).

There is now a new reality that has somewhat dampened the early optimism on just finding and mapping SMFs and then modeling them: the realization that even large-volume landslides may not be as readily identified as previously conceived, as with Grand Banks (Mosher & Piper 2007), or the associated tsunamis as large, as with Trænadjupet (Løvholt et al. 2017). Devastating dual-mechanism tsunamis are a newly realized challenge, most recently flagged by Japan in 2011 and with the newly published research on Messina in 1908 (Schambach et al. 2020b) and Sulawesi (Schambach et al. 2020a). It has been recognized for some time that the Messina earthquake could not have generated the recorded tsunami (Tinti & Armigliato 2003). New numerical modeling in part answers some of the questions here (Schambach et al. 2020b) but not all, as there is an unknown contribution to the tsunami in the north area off of Sicily and Calabria. The MBES bathymetry in the north shows no good evidence for submarine landslides, but earlier suggestions of coastal landslides, perhaps analogous to those in Palu Bay in 2018, might provide the answer. At Sulawesi, the evidence for a dual-mechanism tsunami was apparent from the outset because of the strike-slip fault mechanism; the reports of coastal landslides from the field surveys; and the rapid succession of the sequence of events, earthquake, coastal landslides, and tsunamis (Carvajal et al. 2019). Twenty years earlier, acceptance of this possibility would have been unlikely. Now, there is still controversy over the tsunami mechanisms, but with analogous events, mechanisms previously considered unlikely have become realistic. It is similar with Anak Krakatau. Volcanic collapse is accepted as a possible tsunami mechanism from research in Hawaii and also on the Canary Islands and on the far field hazard to the east coast of the United States (Abadie et al. 2012).

There are now a number of well-studied submarine landslide tsunamis on passive, convergent strike-slip margins and on volcanoes. Over the past 20 years, understanding of landslide mechanisms has advanced significantly. One of the lessons learned is that, compared to earthquakes, a large number of very different landslide mechanisms generate tsunamis. Considering **Figure 1** and comparing the number of landslide events in the context of the length of the oceanic margin where landslides are located, there is a long way to go before their hazard is understood to the level that mitigation can be considered.

FUTURE DIRECTIONS OF RESEARCH

A number of submarine landslide tsunamis have now been identified and well-studied, but still too few are well understood. Based on this review, there are a number of directions to advance our understanding of their mechanisms and their hazard:

- There needs to be a closer collaboration between geoscientists and numerical modelers so that tsunami simulations are well-founded in geological reality.
- There needs to be a greater realization of the limitations of numerical models appropriate to earthquake tsunamis used to simulate landslides.
- There needs to be a greater awareness that landslide tsunami simulations should be validated, either by eyewitness observations and field surveys in the case of historical events or by tsunami sediments for older events.
- As exemplified by Sulawesi, where there is timing information on tsunami impact, this is critical in discrimination mechanisms where there is the possibility of more than one tsunami.
- There needs to be more research on well-studied events to validate existing models.

DISCLOSURE STATEMENT

The author is not aware of any affiliations, memberships, funding, or financial holdings that might be perceived as affecting the objectivity of this review.

ACKNOWLEDGMENTS

Many thanks go to all the colleagues I have worked with on tsunamis, in the field, lab, and office, over the past 20 years. I am responsible, however, for all views and comments in this review. Initially, during the research on the PNG event and for some time afterward, my numerical colleague was Phil Watts, who, unusually for a non-geologist, was one of the first to recognize the tsunami hazard from submarine landslides. Since then, I have worked closely with Stephan Grilli and his numerous students; I thank them all. I also warmly acknowledge the British Geological Survey (formerly the Institute of Geological Sciences), my employer for more than 40 years, for their forbearance, support, and encouragement for a tsunami mechanism that, at first, was thought impossible. For this publication I would also express my appreciation to the Annual Reviews team including Annie Beck as well as Doug Beckner for his work on the figures. I would also acknowledge the European Space Agency for access to the Sentinel-2 data. This review contains satellite imagery from Google Earth, Digital Globe open data for disaster response, and Sentinel-2 cloudless data (**https://s2maps.eu** by EOX IT Services GmbH, containing modified Copernicus Sentinel data 2017 and 2018). The author publishes with the permission of the CEO of the British Geological Survey (United Kingdom Research and Innovation).

LITERATURE CITED

Abadie SM, Harris JC, Grilli ST, Fabre R. 2012. Numerical modeling of tsunami waves generated by the flank collapse of the Cumbre Vieja Volcano (La Palma, Canary Islands): tsunami source and near field effects. *J. Geophys. Res.* 117(C5):C05030

Arikawa T, Muhari A, Okumura Y, Dohi Y, Afriyanto B, et al. 2018. Coastal subsidence induced several tsunamis during the 2018 Sulawesi earthquake. *J. Disaster Res.* 13:sc20181204

Assier-Rzadkieaicz S, Heinrich P, Sabatier PC, Savoye B, Bourillet JF. 2000. Numerical modelling of a landslide-generated tsunami: the 1979 Nice event. *Pure Appl. Geophys.* 157:1707–27

Bao H, Ampuero J-P, Meng L, Fielding EJ, Liang C, et al. 2019. Early and persistent supershear rupture of the 2018 magnitude 7.5 Palu earthquake. *Nat. Geosci.* 12:200–5

Baratta M. 1910. *La Catastrofe Sismica Calabro Messinese (28 Dicembre 1908)*. Rome: Presso Soc. Geograf. Ital.

Bent AL. 1995. A complex double-couple source mechanism for the M_s 7.2 1929 Grand Banks earthquake. *Bull. Seismol. Soc. Am.* 85:1003–20

Billi A, Funiciello R, Minelli L, Faccenna C, Neri G, et al. 2008. On the cause of the 1908 Messina tsunami, southern Italy. *Geophys. Res. Lett.* 35:L06301

Bondevik S, Løvholt F, Harbitz C, Mangerud J, Dawson A, Svendsen JI. 2005. The Storegga Slide tsunami—comparing field observations with numerical simulations. *Mar. Pet. Geol.* 22:195–208

Bondevik S, Mangerud J, Dawson S, Dawson A, Lohne Ø. 2003. Record-breaking height for 8000-year-old tsunami in the North Atlantic. *Eos Trans. AGU* 84:289–93

Bondevik S, Svendsen JI, Mangerud JAN. 1997. Tsunami sedimentary facies deposited by the Storegga tsunami in shallow marine basins and coastal lakes, western Norway. *Sedimentology* 44:1115–31

Boston B, Moore GF, Nakamura Y, Kodaira S. 2017. Forearc slope deformation above the Japan Trench megathrust: implications for subduction erosion. *Earth Planet. Sci. Lett.* 462:26–34

Bryn P, Berg K, Forsberg CF, Solheim A, Lien R. 2005. Explaining the Storegga Slide. *Mar. Pet. Geol.* 22:11–19

Bugge T, Befring S, Belderson RH, Eidvin T, Jansen E, et al. 1987. A giant three-stage submarine slide off Norway. *Geomar. Lett.* 7:191–98

Carvajal M, Araya-Cornejo C, Sepúlveda I, Melnick D, Haase JS. 2019. Nearly instantaneous tsunamis following the *Mw* 7.5 2018 Palu earthquake. *Geophys. Res. Lett.* 46:5117–26

Clague D. 2001. Tsunamis. In *A Synthesis of Geological Hazards in Canada*, ed. GR Brooks, pp. 27–42. Ottawa, Can.: Geol. Surv. Can.

Dawson AG, Long D, Smith DE. 1988. The Storegga Slides: evidence from eastern Scotland for a possible tsunami. *Mar. Geol.* 82:271–76

EMODnet Bathymetry Consort. 2018. EMODnet digital bathymetry (DTM 2018). EMODnet high resolution seabed mapping project, updated Sept. 14. **https://doi.org/10.12770/18ff0d48-b203-4a65-94a9-5fd8b0ec35f6**

Favalli M, Boschi E, Mazzarini F, Pareschi MT. 2009. Seismic and landslide source of the 1908 Straits of Messina tsunami (Sicily, Italy). *Geophys. Res. Lett.* 36:L16304

Felton EA, Crook KAW, Keating BH. 2000. The Hulopoe gravel, Lanai, Hawaii: new sedimentological data and their bearing on the "giant wave" (mega-tsunami) emplacement hypothesis. *Pure Appl. Geophys.* 157:1257–84

Fine IV, Rabinovich AB, Bornhold BD, Thomson RE, Kulikov EA. 2005. The Grand Banks landslide-generated tsunami of November 18, 1929: preliminary analysis and numerical modeling. *Mar. Geol.* 215:45–57

Frederik MC, Adhitama R, Hananto ND, Sahabuddin S, Irfan M, et al. 2019. First results of a bathymetric survey of Palu Bay, Central Sulawesi, Indonesia following the tsunamigenic earthquake of 28 September 2018. *Pure Appl. Geophys.* 176(8):3277–90

Fryer GJ, Watts P, Pratson LF. 2004. Source of the great tsunami of 1 April 1946: a landslide in the upper Aleutian forearc. *Mar. Geol.* 203:201–18

Fujii Y, Satake K, Sakai SI, Shinohara M, Kanazawa T. 2011. Tsunami source of the 2011 off the Pacific coast of Tohoku Earthquake. *Earth Planets Space* 63:55

Fujiwara T, dos Santos Ferreira C, Bachmann AK, Strasser M, Wefer G, et al. 2017. Seafloor displacement after the 2011 Tohoku-oki earthquake in the northern Japan Trench examined by repeated bathymetric surveys. *Geophys. Res. Lett.* 44:11833–39

Geist EL. 2000. Origin of the 17 July 1998 Papua New Guinea tsunami: earthquake or landslide? *Seismol. Res. Lett.* 71:344–51

Glimsdal S, Pedersen GK, Harbitz CB, Løvholt F. 2013. Dispersion of tsunamis: Does it really matter? *Nat. Hazards Earth Syst. Sci.* 13:1507–26

Grauert M, Björck S, Bondevik S. 2001. Storegga tsunami deposits in a coastal lake on Suouroy, the Faroe Islands. *Boreas* 30:263–71

Grigg RW, Jones AT. 1997. Uplift caused by lithospheric flexure in the Hawaiian Archipelago as revealed by elevated coral deposits. *Mar. Geol.* 141:11–25

Grilli ST, Harris JC, Bakhsh TST, Masterlark TL, Kyriakopoulos C, et al. 2013. Numerical simulation of the 2011 Tohoku tsunami based on a new transient FEM co-seismic source: comparison to far- and near-field observations. *Pure Appl. Geophys.* 170:1333–59

Grilli ST, Tappin DR, Carey S, Watt SFL, Ward SN, et al. 2019. Modelling of the tsunami from the December 22, 2018 lateral collapse of Anak Krakatau volcano in the Sunda Straits, Indonesia. *Sci. Rep.* 9:11946

Grilli ST, Vogelmann S, Watts P. 2002. Development of a 3D numerical wave tank for modelling tsunami generation by underwater landslides. *Eng. Anal. Boundary Elem.* 26(4):301–13

Haflidason H, Sejrup HP, Nygård A, Mienert J, Bryn P, et al. 2004. The Storegga Slide: architecture, geometry and slide development. *Mar. Geol.* 213:201–34

Hampton M. 1972. The role of subaqueous debris flow in generating turbidity currents. *J. Sed. Res.* 42:775–993

Hampton MA, Lee HJ, Locat J. 1996. Submarine landslides. *Rev. Geophys.* 34:33–59

Harbitz CB. 1992. Model simulation of tsunamis generated by the Storegga Slides. *Mar. Geol.* 105:1–21

Heezen BC, Ewing M. 1952. Turbidity currents and submarine slumps, and the 1929 Grand Banks earthquake. *Am. J. Sci.* 250:849–73

Hill J, Collins GS, Avdis A, Kramer SC, Piggott MD. 2014. How does multiscale modelling and inclusion of realistic palaeobathymetry affect numerical simulation of the Storegga Slide tsunami? *Ocean Model.* 83:11–25

Hunt JE, Tappin DR, Watt SFL, Susilohadi S, Novellino A, et al. 2021. Submarine observations landslide megablocks show half of the island of Anak Krakatau island failed on December 22nd 2018. *Nat. Commun.* In press

Hurukawa N, Tsuji Y, Waluyo B. 2003. The 1998 Papua New Guinea earthquake and its fault plane estimated from relocated aftershocks. In *Landslide Tsunamis: Recent Findings and Research Directions*, ed. J-P Bardet, F Imamura, CE Synolakis, EA Okal, HL Davies, pp. 1829–41. Boston: Birkhauser

Imamura F, Gica E, Takashi T, Shuto N. 1995. Numerical simulation of the 1992 Flores tsunami: interpretation of tsunami phenomena in northeastern Flores Island and damage at Babi Island. *Pure Appl. Geophys.* 144:555–68

Jamelot A, Gailler A, Heinrich P, Vallage A, Champenois J. 2019. Tsunami simulations of the Sulawesi M_w 7.5 event: comparison of seismic sources issued from a tsunami warning context versus post-event finite source. *Pure Appl. Geophys.* 176:3351–76

Jiang L, Leblond PH. 1992. The coupling of a submarine slide and the surface wave which it generates. *J. Geophys. Res.* 97(C8):12731–44

Jiang L, Leblond PH. 1994. Three-dimensional modelling of tsunami generation due to submarine mudslide. *J. Phys. Oceanogr.* 24:559–73

Johnson C, Mader CL. 1994. Modeling of the 105 Ka Lanai tsunami. *Sci. Tsunami Hazards* 12:33–38

Johnson JM, Satake K. 1997. Estimation of seismic moment and slip distribution of the April 1, 1946 Aleutian tsunami earthquake. *J. Geophys. Res.* 102(B6):11765–74

Kanamori H. 1972. Mechanism of tsunami earthquakes. *Phys. Earth Planet. Inter.* 6:346–59

Kawamura K, Sasaki T, Kanamatsu T, Sakaguchi A, Ogawa Y. 2012. Large submarine landslides in the Japan Trench: a new scenario for additional tsunami generation. *Geophys. Res. Lett.* 39:L05308

Kawata Y, Benson BC, Borrero JL, Davies HL, De Lange WP, et al. 1999. Tsunami in Papua New Guinea was as intense as first thought. *Eos Trans. AGU* 80:101104–5

Kulikov EA, Rabinovich AB, Thomson RE, Bornhold BD. 1996. The landslide tsunami of November 3, 1994, Skagway Harbor, Alaska. *J. Geophys. Res.* 101(C3):6609–15

Lay T. 2018. A review of the rupture characteristics of the 2011 Tohoku-oki Mw 9.1 earthquake. *Tectonophysics* 733:4–36

Leblond PH, Jones A. 1995. Underwater landslides ineffective at tsunami generation. *Sci. Tsunami Hazards* 13:25–26

Lee HJ, Kayen RE, Gardner JV, Locat J. 2003. Characteristics of several tsunamigenics submarine landslides. In *Submarine Mass Movements and Their Consequences: 1st International Symposium*, ed. J Locat, J Mienert, pp. 357–66. Dordrecht, Neth.: Kluwer

Liu PL, Higuera P, Husrin S, Prasetya GS, Prihantono J, et al. 2020. Coastal landslides in Palu Bay during 2018 Sulawesi earthquake and tsunami. *Landslides* 17:2085–98

López-Venegas AM, Brink UST, Geist EL. 2008. Submarine landslide as the source for the October 11, 1918 Mona Passage tsunami: observations and modeling. *Mar. Geol.* 254:35–46

Løvholt F, Bondevik S, Laberg JS, Kim J, Boylan N. 2017. Some giant submarine landslides do not produce large tsunamis. *Geophys. Res. Lett.* 44:8463–72

Løvholt F, Pedersen G, Harbitz CB, Glimsdal S, Kim J. 2015. On the characteristics of landslide tsunamis. *Philos. Trans. R. Soc. A* 373:20140376

Løvholt F, Schulten I, Mosher D, Harbitz C, Krastel S. 2018. Modelling the 1929 Grand Banks slump and landslide tsunami. *Geolog. Soc. Lond. Spec. Publ.* 477:315–31

MacInnes BT, Gusman AR, Leveque RJ, Tanioka Y. 2013. Comparison of earthquake source models for the 2011 Tohoku event using tsunami simulations and near-field observations. *Bull. Seismol. Soc. Am.* 103:1256–74

Marani MP, Gamberi F, Bortoluzzi G, Carrara G, Ligi M, Penitenti D. 2004. Seafloor bathymetry of the Ionian Sea. In *From Seafloor to Deep Mantle: Architecture of the Tyrrhenian Backarc Basin*, Vol. 44. ed. MP Marani, F Gamberi, E Bonatti, plate 3. Rome: APAT

McMurtry GM, Fryer GJ, Tappin DR, Wilkinson IP, Williams M, et al. 2004a. Megatsunami deposits on Kohala volcano, Hawaii, from flank collapse of Mauna Loa. *Geology* 32:741–44

McMurtry GM, Watts P, Fryer GJ, Smith JR, Imamura F. 2004b. Giant landslides, mega-tsunamis, and paleo-sea level in the Hawaiian Islands. *Mar. Geol.* 203:219–33

Moore AL. 2000. Landward fining in onshore gravel as evidence for a late Pleistocene tsunami on Molokai, Hawaii. *Geology* 28:247–50

Moore GW, Moore JG. 1988. Large-scale bedforms in boulder gravel produced by giant waves in Hawaii. *Geol. Soc. Am. Spec. Pap.* 229:101–10

Mosher DC, Piper DJW. 2007. Analysis of multibeam seafloor imagery of the Laurentian Fan and the 1929 Grand Banks landslide area. In *Submarine Mass Movements and Their Consequences: 3rd International Symposium*, ed. V Lykousis, D Sakellariou, J Locat, pp. 77–88. Dordrecht, Neth.: Springer

Muhari A, Imamura F, Arikawa T, Hakim AR, Afriyanto B. 2018. Solving the puzzle of the September 2018 Palu, Indonesia, tsunami mystery: clues from the tsunami waveform and the initial field survey data. *J. Disaster Res.* 13:sc20181108

Murty TS. 1977. Seismic sea waves—tsunamis. *Bull. Fish. Res. Board Can.* 198:337

Nakamura Y, Fujiwara T, Kodaira S, Miura S, Obana K. 2020. Correlation of frontal prism structures and slope failures near the trench axis with shallow megathrust slip at the Japan Trench. *Sci. Rep.* 10:11607

Nakata K, Katsumata A, Muhari A. 2020. Submarine landslide source models consistent with multiple tsunami records of the 2018 Palu tsunami, Sulawesi, Indonesia. *Earth Planets Space* 72:44

Newman AV, Okal EA. 1998. Teleseismic estimates of radiated seismic energy: the E/M_0 discriminant for tsunami earthquakes. *J. Geophys. Res.* 103(B11):26885–98

Okada Y. 1985. Surface deformation due to shear and tensile faults in a half-space. *Bull. Seismol. Soc. Am.* 75:1135–54

Omori F. 1909. Preliminary report on the Messina-Reggio earthquake of Dec. 28, 1908. *Bull. Imp. Earthq. Investig. Comm.* 3(2):37–45

Pakoksung K, Suppasri A, Imamura F, Athanasius C, Omang A, Muhari A. 2019. Simulation of the submarine landslide tsunami on 28 September 2018 in Palu Bay, Sulawesi Island, Indonesia, using a two-layer model. *Pure Appl. Geophys.* 176:3323–50

Piper DJW, Shor AN, Clarke JEH. 1988. The 1929 Grand Banks earthquake, slump and turbidity current. *Geol. Soc. Am. Spec. Pap.* 229:77–92

Plafker G, Kachadoorian R, Eckel EB, Mayo LR. 1969. *Effects of the earthquake of March 27, 1964 on various communities*. Prof. Pap. 542-G, US Geol. Surv., Washington, DC

Platf. Promot. Early Warn. 2006. Tsunami: What is tsunami? *International Strategy for Disaster Reduction*. **https://www.unisdr.org/2006/ppew/tsunami/what-is-tsunami/backinfor-brief.htm**

Priyanto WS, Hunt JE, Hanif M, Tappin DR, Permana H, et al. 2021. Bathymetry and shallow seismic imaging of the 2018 flank collapse of Anak Krakatau. *Front. Earth Sci.* 8:649

Rubin KH, Fletcher CH, Sherman C. 2000. Fossiliferous Lana'i deposits formed by multiple events rather than a single giant tsunami. *Nature* 408:675–81

Ruff L, Kamamori H. 1980. Seismicity and the subduction process. *Phys. Earth Planet. Inter.* 23:240–52

Ruffman A, Hann V. 2006. The Newfoundland tsunami of November 18, 1929: an examination of the twenty-eight deaths of the "South Coast Disaster." *Nfld. Labrador Stud.* 21:1719–26

Ryan WBF, Heezen BC. 1965. Ionian sea submarine canyons and the 1908 Messina turbidity current. *Geol. Soc. Am. Bull.* 76:915–32

Schambach L, Grilli ST, Tappin DR. 2020a. New high-resolution modeling of the 2018 Palu tsunami, based on supershear earthquake mechanisms and mapped coastal landslides, supports a dual source. *Front. Earth Sci.* 8:627

Schambach L, Grilli ST, Tappin DR, Gangemi MD, Barbaro G. 2020b. New simulations and understanding of the 1908 Messina tsunami for a dual seismic and deep submarine mass failure source. *Mar. Geol.* 421:106093

Schulten I, Mosher DC, Krastel S, Piper DJW, Kienast M. 2018. Surficial sediment failures due to the 1929 Grand Banks Earthquake, St Pierre Slope. *Geol. Soc. Lond. Spec. Publ.* 477:583–96

Smith DE, Foster IDL, Long D, Shi S. 2007. Reconstructing the pattern and depth of flow onshore in a palaeotsunami from associated deposits. *Sediment. Geol.* 200:362–71

Socquet A, Hollingsworth J, Pathier E, Bouchon M. 2019. Evidence of supershear during the 2018 magnitude 7.5 Palu earthquake from space geodesy. *Nat. Geosci.* 12:192–99

Solheim A, Bryn P, Sejrup HP, Mienert J, Berg K. 2005. Ormen Lange—an integrated study for the safe development of a deep-water gas field within the Storegga Slide Complex, NE Atlantic continental margin; executive summary. *Mar. Pet. Geol.* 22:1–9

Song X, Zhang Y, Shan X, Liu Y, Gong W, Qu C. 2019. Geodetic observations of the 2018 *Mw* 7.5 Sulawesi earthquake and its implications for the kinematics of the Palu Fault. *Geophys. Res. Lett.* 46:4212–20

Stearns HT. 1978. *Quaternary Shorelines in the Hawaiian Islands*. Honolulu, HI: Bernice P. Bishop Mus.

Stein S, Okal EA. 2007. Ultralong period seismic study of the December 2004 Indian Ocean earthquake and implications for regional tectonics and the subduction process. *Bull. Seismol. Soc. Am.* 97(1A):S279–95

Sweet S, Silver EA. 2003. Tectonics and slumping in the source region of the 1998 Papua New Guinea tsunami from seismic reflection images. In *Landslide Tsunamis: Recent Findings and Research Directions*, ed. J-P Bardet, F Imamura, CE Synolakis, EA Okal, HL Davies, pp. 1945–68. Boston: Birkhauser

Synolakis CE, Bardet J-P, Borrero JC, Davies HL, Okal EA, et al. 2002. The slump origin of the 1998 Papua New Guinea tsunami. *Proc. R. Soc. Lond. Ser. A: Math. Phys. Eng. Sci.* 458:763–89

Tanioka Y, Satake K. 1996. Tsunami generation by horizontal displacement of ocean bottom. *Geophys. Res. Lett.* 23:861–64

Tappin DR. 2010. Digital elevation models in the marine domain: investigating the offshore tsunami hazard from submarine landslides. *Geol. Soc. Lond. Spec. Publ.* 345(1):81–101

Tappin DR. 2017. Tsunamis from submarine landslides. *Geol. Today* 33:190–200

Tappin DR. 2020. Chemosynthetic seep communities triggered by seabed slumping off of northern Papua New Guinea. In *Seafloor Geomorphology as Benthic Habitat*, ed. PT Harris, E Baker, pp. 875–87. Cambridge, MA: Elsevier

Tappin DR, Grilli ST, Harris JC, Geller RJ, Masterlark T, et al. 2014. Did a submarine landslide contribute to the 2011 Tohoku tsunami? *Mar. Geol.* 357:344–61

Tappin DR, Matsumoto T, Watts P, Satake K, McMurtry GM, et al. 1999. Sediment slump likely caused 1998 Papua New Guinea tsunami. *Eos Trans. AGU* 80:329–40

Tappin DR, Watts P, Grilli ST. 2008. The Papua New Guinea tsunami of 17 July 1998: anatomy of a catastrophic event. *Nat. Hazards Earth Syst. Sci.* 8:243–66

Tappin DR, Watts P, McMurtry GM, Lafoy Y, Matsumoto T. 2001. The Sissano, Papua New Guinea tsunami of July 1998—offshore evidence on the source mechanism. *Mar. Geol.* 175:1–23

Tinti S, Armigliato A. 2003. The use of scenarios to evaluate the tsunami impact in southern Italy. *Mar. Geol.* 199:221–43

Ulrich T, Vater S, Madden EH, Behrens J, Van Dinther Y, et al. 2019. Coupled, physics-based modeling reveals earthquake displacements are critical to the 2018 Palu, Sulawesi tsunami. *Pure Appl. Geophys.* 176:4069–109

Walter TR, Haghshenas-Haghighi M, Schneider FM, Coppola D, Motagh M, et al. 2019. Complex hazard cascade culminating in the Anak Krakatau sector collapse. *Nat. Commun.* 10:4339

Watts P. 1998. Wavemaker curves for tsunamis generated by underwater landslides. *J. Waterw. Port Coast. Ocean Eng.* 124:127–37

Watts P, Grilli ST, Kirby JT, Fryer GJ, Tappin DR. 2003. Landslide tsunami case studies using a Boussinesq model and a fully nonlinear tsunami generation model. *Nat. Hazards Earth Syst. Sci.* 3:391–402

Yamazaki Y, Cheung KF, Lay T. 2018. A self-consistent fault slip model for the 2011 Tohoku earthquake and tsunami. *J. Geophys. Res. Solid Earth* 123:1435–58

Yeh H, Imamura F, Synolakis C, Tsuji Y, Liu P, Shi S. 1993. The Flores Island tsunamis. *Eos Trans. AGU* 74:369–73

Yeh H, Liu P, Briggs M, Synolakis C. 1994. Propagation and amplification of tsunami at coastal boundaries. *Nature* 372:353–55

Zengaffinen T, Løvholt F, Pedersen G, Harbitz CB. 2020. Effects of rotational submarine slump dynamics on tsunami genesis—new insight from idealized models and the 1929 Grand Banks event. *Geol. Soc. Lond. Spec. Publ.* 500:41–61

Annual Review
of Earth and
Planetary Sciences
Volume 49, 2021

Contents

Errata

An online log of corrections to *Annual Review of Earth and Planetary Sciences* articles may be found at http://www.annualreviews.org/errata/earth